MARMARA UNIVERSITY
INSTITUTE FOR GRADUATE STUDIES IN PURE AND APPLIED SCIENCES

AMMONIUM ION REMOVAL IN SEGREGATED FLUIDIZED BEDS: EFFECTS OF FLOW RATE AND NUMBER OF SEGREGATED LAYERS

GÜLAY ARSLAN
(524312701)

MASTER THESIS
Department of Environmental Engineering

ADVISOR
Assist. Prof. Elif SOYER

ISTANBUL, 2015

ACKNOWLEDGEMENT

Firstly I wish to express my deepest gratitude to my thesis supervisor Assist. Prof. Elif SOYER, for her interest and support throughout the development of this my thesis and for tolerance that she showed during the writing period of this thesis.

I would like to thank my jury members Prof. Dr. Ömer AKGİRAY and Assoc. Prof. Dr. Ayşe ÇEÇEN ERBİL for spending their valuable time for my thesis.

I would also like to thank Assist. Prof. Esra ERDİM for her kind guidance and helps.

I am also grateful to my friends, Özge ÇAĞLAYAN, Kübra TEMİZ, Zeynep YÜCESOY ÖZKAN, Çiğdem KALKAN AKTAN, Alper BAYRAKDAR, Gül Gülenay HACIOSMANOĞLU, Elif Gökçe UÇAR, Hatice TANER and Hatice YEŞİL for their friendship, understanding and endless support throughout this study.

I am also grateful to Özlem KAPLAN for her kind guidance and help while I was doing my thesis.

I would like to express my deep appreciation to Recep Önder SÜRMELİ for his advice and help while I was doing my thesis.

Finally, I would like to express my thankfulness to my mother, father, sister, brother, my fiancé Onur and his family for their incredible support, continual encouragement, understanding, patience and their never ending love.

Thank you for being with me all the time.

December, 2015 **Gülay ARSLAN**

TABLE OF CONTENTS

AMMONIUM ION REMOVAL IN SEGREGATED FLUIDIZED BEDS: EFFECTS OF FLOW RATE AND NUMBER OF SEGREGATED LAYER

ABSTRACT

Removal of ammonium ion from water in fluidized bed ion exchange columns of clinoptilolite was investigated in this research. Objectives of the study were (i) investigation of the use of clinoptilolite in monodispersed and polydispersed fluidized beds for the removal of ammonium ion, (ii) comparison of the performances obtained with different composition of mixed beds, and (iii) investigation of the effect of increase in flow rate (bed expansion and expanded bed porosity).

Four different fractions of clinoptilolite were prepared by sieving and by conditioning the surface of particles using sodium chloride. Four different monodispersed fluidized beds were operated at several different flow rates to investigate the effects of particle size and fluidization rate on ammonium exchange performance. 7 different compositions of polydisperse fluidized beds (four different compositions of binary beds, two different ternary beds and a bed containing all particle sizes together) were operated at two different flow rates to determine the effects of average particle size and mixing behaviors on ammonium exchange capacity. Same set of experiments were conducted at the same operating conditions to find the values of overall mass transfer coefficients.

All results of the experiments performed were evaluated using parameters: (i) ratio of breakthrough capacity to total (or exhaustion capacity), (ii) bed usage rate, and (iii) fractional capacity.

The ratio of breakthrough capacity to total capacity is increases when the column is efficiently. On the other hand, an improved performance is represented with a decreased value of bed usage rate. Increase in fluidization rate and employing particle mixtures of different sizes in the ion exchange bed were found to improve separation efficiencies of ammonium ion in clinoptilolite beds.

Keywords: ammonium ion, ion exchange, clinoptilolite, zeolite, fluidization, monodisperse and polydisperse particle systems

January, 2016 **Gülay ARSLAN**

TABAKALAŞMIŞ AKIŞKAN YATAKLI REAKTÖRLERDE AMONYUM İYONU GİDERİMİ : AKIŞKANLAŞMA HIZI VE TABAKA SAYISI ETKİSİ

ÖZET

Klinoptilolit içeren akışkan yataklarda amonyum iyonu gideriminin araştırıldığı bu çalışmanın amaçları arasında: (i) amonyum iyonu değişimi için homojen parçacık boyutu içeren tek tabakalı yataklar ve farklı tane boyutlarını bir arada içeren akışkan yatakların incelenmesi, (ii) ikili, üçlü ve daha çok sayıda farklı tane boyutu içeren karışık yatakların amonyak giderim performanslarının karşılaştırılması ve (iii) akışkanlaşma hızının akışkan yatak performansına etkilerinin araştırılması bulunmaktadır.

Dört farklı klinoptilolit fraksiyonu elenerek hazırlanmış ve tane yüzeyleri sodyum klorür ile temas ettirilerek modifiye edilmiştir. Dört farklı tek tabakalı üniform boyut dağılımında akışkan yatak farklı akışkanlaşma hızlarında işletilmiş ve tane boyutu ile akışkanlaşma hızının amonyak değişim performansları üzerine etkileri araştırılmıştır. Yedi farklı kompozisyonda tane boyutu karışımlarını içeren (dört farklı kompozisyonda ikili karışım, 2 farklı kompozisyonda üçlü karışım ve tüm parçacık boyutlarının karışım olarak incelendiği akışkan yatak) akışkan yataklar üzerinde deneyler yürütülmüş ve iki farklı akışkanlaşma hızı, farklı tane boyutu karışım kombinasyonlarının iyon değişimi performansı üzerine etkileri incelenmiştir. Aynı işletme koşulları ve parçacık kompozisyonlarında deneyler gerçekleştirilerek kütle transferi katsayıları tespit edilmiştir.

Elde edilen tüm sonuçlar, (i) kırılma noktası kapasitesinin toplam kapasiteye oranı, (ii) yatak kullanım hızı, (iii) fraksiyonel kapasite kullanılarak değerlendirilmiştir.

Kırılma noktası kapasitesinin toplam yatak kapasitesine oranı akışkanlaşma kolonun verimli bir şekilde kullanımı ile artmaktadır. Bununla birlikte, akışkan yatağın daha verimli kullanıldığının bir göstergesi de azalan yatak kullanım hızları olmaktadır. Artan

akışkanlaşma hızları ve akışkan yatak içerisinde farklı tane boyutlarında klinoptilolit parçacıkların bir arada karışım olarak kullanılmasının amonyak iyon değişim performansını arttırdığı gözlenmiştir.

Anahtar kelimeler: amonyum iyonu, iyon değişimi, klinoptilolit, zeolite, akışkanlaşma, homojen ve tane boyut dağılımına sahip sistemler

Ocak, 2016 **Gülay ARSLAN**

SYMBOLS

cm	: Centimeter
D	: Day
g	: Gram
h	: Hour
L	: Liter
mg	: milligram
m^2	**:** Meter square
m^3	**:** Cubic meter
NH_4Cl	: Ammonium Chloride
NaCl -	: Sodium Chloride
Sec	: Second
%	**:** Percentage
µm	**:** Micro Meter
°C	**:** Degree Celsius

ABBREVIATIONS

A : Area (m^2)

BUR : Bed Usage Rate

BVs : Settled Bed Volume

C_0 : Ammonium Ion Feed

C_{feed} : Concentration in Feed (mg/L)

d_1 : 250-355 μm

d_2 : 355-425 μm

d_3 : 425-500 μm

d_4 : 500-600 μm

dpi : Particle Size fraction

dp : weight averaged particle size

E : Bed Expansion

F : Fractional Capacity

H : Fluidized bed height (cm)

He : Expanded bed height (cm)

Hsett : Settled Bed Height (cm)

ISA : Ionic Strength Adjustor

k_L : Mass Transfer Coefficient

M : Mass of particles (g)

MD : Mechanical Dispertion

tc : Empty Bed Contact Time

V : Linear (superficial) Velocity

Vi : Interstitial Velocity

X : Breakthrough Capacity (mg NH_4^+)

Xi : Weight fraction of particle size d_{pi}

ρ_p : Specific Gravity of Clinoptilolite

ϵ : Voidage

Q : Flow Rate

WWT : Waste Water Treatment

LIST OF FIGURES

LIST OF TABLES

1. INTRODUCTION

1.1.Background

Domestic and industrial wastewaters contain considerable amount of ammonia nitrogen (NH_3/NH_4^+-N). Ammonia nitrogen is separated and/or treated before discharging these types of wastewaters into surface waters and receiving water bodies to prevent eutrophication. In certain cases such as supplying drinking water from surface water containing high levels of ammonium ion, several types of removal methods should be considered as well. Thus, the development of an efficient removal technology for ammonium ion receives great attention.

1.2. Objective of the Study

This study is focused on removal of ammonium ion from water in ion exchange columns of clinoptilolite which were operated in fluidized mode.
Objectives of this research are:

- To investigate the use of clinoptilolite in monodispersed and polydispersed fluidized beds for the removal of ammonium ion.
- To compare the performance of different composition of mixed beds.

To investigate the effect of increase in flow rate (bed expansion and expanded bed porosity).

1.3. Literature Review

Turkish clinoptilolite from Balikesir, Bigadic, was used for the removal of ammonium ion (Demir et al., 2002). Particle sizes employed in batch equilibrium studies were 0.125-1.00 and 1.00-2.00 mm. Capacities of exchange were reported as 0.57 meq/g and 0.38 meq/g for fine and coarse particles, respectively. Same particle size fractions were used in column studies where the ion exchange beds were operated in fixed bed mode. Exhaustion and breakthrough conditions were improved when the clinoptilolite beds were regenerated using sodium chloride solutions.
In another study, Karadag et al., (2006) investigated the removal of ammonium ion using Turkish clinoptilolite. Experimental work includes a batch experiment technique

where the zeolites at a particle size between 1.0-1.4 mm were equilibrated with an initial ammonium ion concentration in the range of 25-250 mg/L. Exchange capacity of Turkish clinoptilolite was to be around 8 mg/g.

In another study, researches Saltali et al. (2007) investigated the exchange potential of a different type of Turkish zeolite (Sivas, Yildizeli region) by conducting similar type of batch experiments. Particle size of zeolite used in their study was 75 μm. Maximum amount of NH_4^+ exchanged by zeolite was found to be around 10 mg/g.

Wang et al. (2007) reported that natural clinoptilolite contacted with sodium hydroxide before hydrothermal reaction to prepare modified zeolites, exhibited higher uptake capacity (19.29 mg/g) compared to natural clinoptilolite particles in pristine form (10.49 mg/g). 75 μm zeolite particles were used in batch equilibrium studied.

Monvalto et al. (2012) evaluated the studies regarding the application of zeolites in anaerobic digestion processes where high levels of nitrogen compounds prevent process kinetics and cause inhibition. Natural zeolites used as support material for microorganisms in different reactor configurations such as fixed or fluidized beds were also reviewed.

Removal of ammonia nitrogen by modified clinoptilolite in the presence of phosphates was studied (Huo et al., 2012) on synthetic waters prepared from ammonium chloride (ammonia nitrogen concentration was 25 mg/L) and dipotassium hydrogen phosphate (phosphate concentration was 5 mg/L). Clinoptilolite used in the study had a particle size of 50-74 μm and modified by contacting with sodium chloride and ferric chloride prior to a thermal processing at 200 ^oC. An equilibrium time of 150 min resulted in an uptake by modified clinoptilolite of about 2.7 mg/g.

Ion exchange of ammonium ion from synthetically prepared solutions as well as wastewaters obtained from a hen slaughterhouse was investigated experimentally (Arslan and Veli, 2012). Four types of zeolites were employed in experiments. These were Aqua-Multalite (75 μm in size), Manisa-Gordes clinoptilolite (65 μm), zeolite 13X (2 μm) and zeolite 4A (5 μm). Highest removal rates were reported for Zeolite 13X (5.10 mg/g and 4.21 mg/g for synthetic and diluted slaughterhouse wastewater, respectively).

Adsorption mechanisms, namely particle diffusion and film diffusion, were studied experimentally for exchange of ammonium ion on natural and sodium chloride modified

zeolites (Lin et al., 2013). Sodium content after modification was 192% higher than the sodium content of natural zeolite. It was found that modification had also increased specific surface and pore diameter of zeolite. Film diffusion properties had been found to improve following NaCl modification. Maximum adsorption capacity of modified zeolite was reported as 14.3 mgN/g.

Alshameri et al. (2014) investigated the use of Yemeni natural zeolite for the removal of ammonium ion in a batch system. Zeolites were used in natural form as well as after modifying their surface with sodium. Particle size range of zeolite used in the study was 62-74 μm. Ammonium exchange capacities of surface modified and pristine zeolites were found as 11.18 mg/g and 8.29 mg/g, respectively.

Zhou and Boyd (2014) studied the removal efficiency of total ammonia nitrogen by two types of natural zeolites (mordenite). Zeolite samples used had a size range of 50-800 μm. Adsorption efficiencies of both samples were found to be 8.7 mgTAN/g (equilibrated with 200 mg/L total ammonia nitrogen concentration). Decreased removal efficiencies were reported when zeolite samples were tested in aquariums where high levels of ammonium and salinity together presents.

Liao et al (2015) employed a combined use of powdered activated carbon and powdered zeolite to improve separation efficiency of ammonium ion in micro-polluted raw water. River water, which includes micro pollutants, was spiked with NH_4Cl to increase the levels of ammonium ion originally present (2.70 mg/L). Particle sizes of zeolite and powdered activated carbon were about 75 and 500 μm, respectively. Dosing of zeolite and powdered activated carbon together at the beginning of flocculation found to efficient for achieving high level of removal rates for turbidity, ammonium ion and organic contaminants.

Huang et al (2015) investigated the exchange of ammonium ion from swine wastewater by employing zeolites with a size range of 300-500 μm. Effectiveness of the process was tried to be increased by applying chlorination for regeneration at a stage wise operation: ion exchange run at 120 min of duration followed by 10 min of regeneration conducted at the same reactor.

Zeolites synthesized from fly ash (as waste material generated from electric power plants) were used in immobilization of ammonium (Ji et al., 2015). Two types of fly ash, high-calcium and low-calcium, were tested by conducting batch equilibrium

studies. Low-calcium zeolite was found to have higher ammonium immobilization capacity than high-calcium zeolite.

Two types of Australian natural zeolites were used for the removal of ammonium ion in a recent study (Millar et al., 2016). It was reported that, a pretreatment using sodium hydroxide following the contact with an acid improves ammonium exchange efficiency. Removal mechanisms of high levels of ammonium ion from swine wastewater were investigated using a natural zeolite without modification and after modifying zeolite with magnesium oxide, MgO (Guo, 2015). Ammonium adsorption capacity of the new synthesized zeolite was reported as 24.9 mg/g.

Haji et al (2015) investigated the use of several commercially available zeolites for the removal of ammonium ion from aqueous solutions. These zeolites were Beta, Y, 4A, and 13X. Na-Y and Na-X zeolites were found to be the best types since they have love Si/Al ratio, high surface area and large pore size. Exchange capacity was reported as 25.7 mg/g. Thermal regeneration alone, contacting with a saline water alone and the combination of both were tested. Combination of the two regeneration methods was reported as the best effective method among all.

Expanded bed adsorption technology is a solid-liquid separation process and is used for removal and/or purification of substances (Lin et al., 2015). Process efficiency depends on several factors including size distribution of adsorbent/resin particles, local bed voidage along the bed height and mass transfer kinetics.

Erbil et al (2011) studied the removal of ammonium ion with a natural zeolite in monodispersed and segregated fluidized beds. It was found that using two non-mixing size fractions of clinoptilolite in a fluidization column improves the column efficiencies measured in terms of breakthrough capacity / total capacity. Size fractions used in the study were 250-350, 500-600 and 840-1000 μm.

Process efficiencies of a fixed and a fluidized bed for the removal of heavy metals (manganese, zinc and chromium) by using clinoptilolite were investigated in a recent study (Stylianou et al., 2015). Particle size of the clinoptilolite was 90-180 μm. Experimental columns employed in ion exchange experiments were different (inner diameters of the exchange columns were 4.4 and 2 cm for fluidized bed and for the fixed bed, respectively). Volume of fluidized bed and fixed bed were 331 and 63 mL,

respectively. Both columns were operated at the same flowrate given as 12.5 BV/h. Expanded bed porosity in the fluidized column was reported as 0.715. Removal efficiencies of both column were evaluated only in terms of bed volume of water treated until breakthrough point at this only one flow rate. As expected, shortened breakthrough times were reported for fluidized beds than the breakthrough times obtained with fixed columns.

Chaudhari and Deshmukh (2015) studied the effects of operating a removal and recovery system in fluidization mode for Palladium (II) separation from wastewaters. Authors reported that the fluidization method gives better results than the results obtained with batch operation. Removal rates could be increased up to 100% in very short residence times compared to reaction times required in batch operation. Fluidization was also found to increase solid-liquid mass transfer rates and mass transfer coefficients. It was concluded that these two effects, high residence times together with increased mass transfer coefficients, had resulted in an overall increase in rates of exchange and process performance.

Kalaruban et al (2016) investigated the efficiencies of removal nitrate from water using two types of resin, a commercial ion exchange resin (Dowex 21K XLT) and its surface modification using iron (incorporating iron into commercial resin). Researchers had conducted experiments of both batch equilibrium and fluidized bed adsorption experiments. Fluidized bed adsorption capacities of both commercial and modified resin were found to decrease than the capacities obtained with batch equilibrium studies. This was an expected situation, because in a fluidized bed adsorption mode residence time of nitrate is shorter compared to a batch operation where the equilibrium can be reached in longer durations and maximum removal efficiencies can be achieved.

2. MATERIAL AND METHOD

2.1. Experimental Setup

Ammonium ion exchange behavior of a natural zeolite, clinoptilolite was performed in a fluidization column. Plexyglass column had an inner diameter of 21.9 mm and a height of 100 cm. NH_4^+ solution was prepared in each set of experiment using ammonium chloride, NH_4Cl and deionized water. Synthetically prepared feed solution was stored in a 100 L tank and kept continuously mixed using a flow through working submerged pump. Another submerged pump supplied the feed solution to the fluidization column. A pipeline with two valves (one line supplying the required flows to the system and the other is recirculating the excess flow into the feed tank) was used in order to arrange flow rates needed fluidization of clinoptilolite bed at constant rates. Experimental setup is illustrated in Figure 2.1. Samples from column effluent were taken in every 5 minutes during the first 30 minutes to 1 hour of a run. Then, sampling from the effluent was employed in every 10-15 minutes. Temperature of influent and column effluent were recorded. Samples from influent were also taken to ensure that a constant and 25 mg/L ammonium ion concentration was supplied to the column. The port that should be opened and a continuous effluent flow obtained was determined at the beginning of each experiment since the point of sampling (effluent) was different at different rates of flow and for different types of particle size compositions.

Figure 2.2 shows the picture of experimental system. Plexyglass fluidization column, feed water tank, influent valves and effluent container can be seen from the picture.

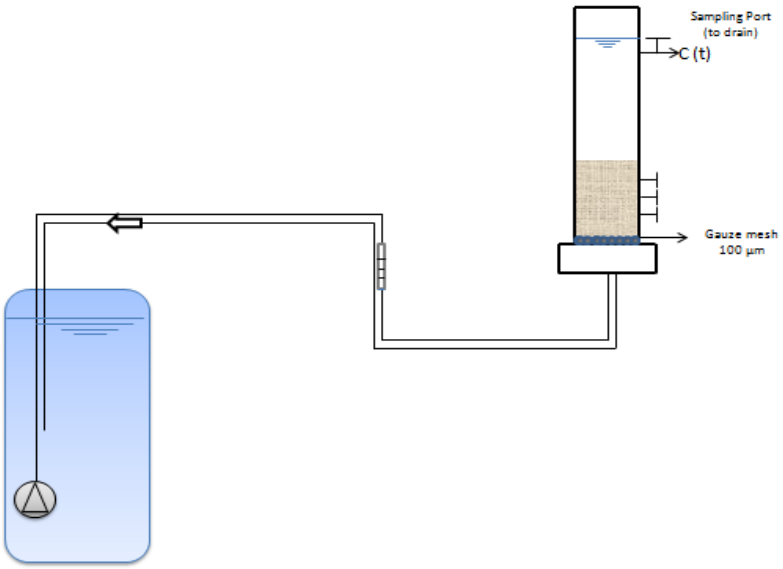

Figure 2.1. A schematic view of the experimental system.

Figure 2.2. Experimental setup used during the fluidized bed ion exchange studies.

2.2. Preparation of Clinoptilolite

A natural zeolite, clinoptilolite, with a chemical formula of $(Na_4K_4).(Al_8Si_{40}).O_{96}24H_2O$ was used in experiments. Clinoptilolite was obtained from a company marketing zeolites from Balikesir, Bigadic region. Particle fractions of clinoptilolite were prepared by a sieving procedure which involves first the sieving with a sieve shaker (Ro-Tap

Sieve Shaker, Retsch AS200) and then a manuel wet sieving process. Wet sieving step was required because of small particle sizes and inefficient sieving during dry sieving process. Sieve shaker and standard sieves used were shown in Figure 2.3 and Figure 2.4. Standard sieves employed in this study had appertures of 600, 500, 425, 355 and 250 μm.

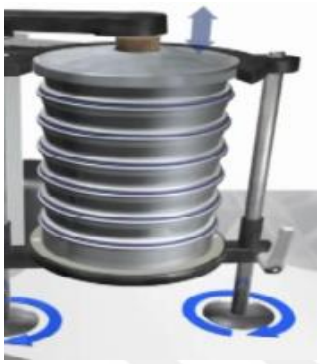

Figure 2.3. Ro-tap sieve shaker (Retsch AS200).

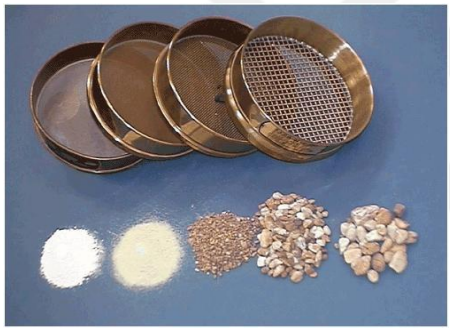

Figure 2.4. Standard sieves

Size fractions prepared were given in Table 2.1. Each particle size fraction was washed, oven dried (103-105 ^{o}C) and stored before further processing.

Table 2.1. Prepared fractions of clinoptilolite by sieving.

Particle size fraction	**Sieve size range (μm)**	**Average sieve size (μm)**
d_1	250-355	303
d_2	355-425	390
d_3	425-500	463
d_4	500-600	550

2.3. Conditioning Studies

NaCl solution was used for conditioning. Each fraction was conditioned with 1 M NaCl solution to convert the natural clinoptilolite into Na form. Each fraction was contacted with NaCl solution for about 24 hours at 20-25 ^{o}C in a shaker working at 150 rpm (Figure 2.5). Approximately 30 g of clinoptilolite was contacted with 250 mL NaCl during these step. Another fresh solution of 1 M NaCl was replaced after 1 day and contacted for several additional hours to ensure that each particle size had Na exchange sites. After conditioning with NaCl, clinoptilolite particles were rinsed with deionized water, dried at 103-105 ^{o}C and stored in a dessicator prior to use.

Figure 2.5. Conditioning of clinoptilolite particles with 1 M NaCl.

Same steps were followed in regeneration of used clinoptilolite.

2.4. Measurement of Ammonium Ion Concentration

Ammonium ion solutions were prepared by diluting the stock solutions prepared by dissolving ammonium chloride in deionized water. 25 mg/L NH_4^+ solutions were prepared and used in fluidization experiments. Deionized water produced from a reverse osmosis system was employed in this study since liquid solutions of large volumes required in each run.

An ammonia selective electrode and an ion meter were used for measurements of ammonium ion (Thermo Orion Advanced Ion Selective Electrode Meter 720A$^+$). Ion meter was calibrated with standard solutions prepared from a stock solution of NH_4^+-N. After calibration to the desired range of concentration, samples taken from both influent and effluent were measured.

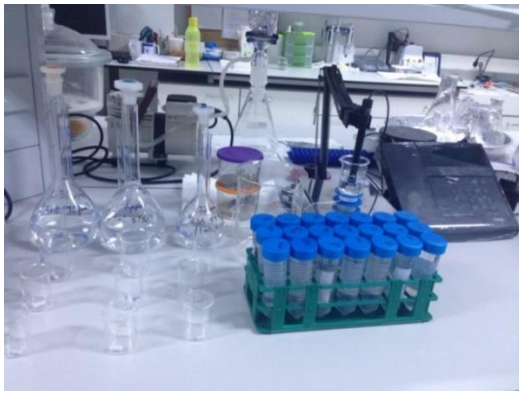

Figure 2.6. Thermo Orion Advanced Ion Selective Meter.

2.5. Particle Mixtures Used in Fluidized Bed Ion Exchange Experiments

Monodispersed and polydispersed particles of clinoptilolite were used in fluidized bed ion exchange experiments. Four different particle size range of clinoptilolite was used in monodispersed fluidized bed experiments. These were listed in Table 2.1 above. Seven different particle size range of clinoptilolite mixtures were prepared for polydispersed fluidized bed experiments. These include four types of binary particle system, two types of ternary particle system and one particle mixture including all particle sizes together. Mass of clinoptilolite bed was constant and 50 grams in all runs. For polydisperse particle systems combinations were prepared by taking equal amounts from each particle size. For a binary particle bed each particle fraction had a mass of 25 g, whereas for the ternary bed particle fractions with a mass of 16.667 g were mixed. For the bed composed of all four size range of particles, every fraction had a mass of 12.5 g and the total bed weight was 50 g.

All of these eleven particle bed compositons are shown in Figure 2.9. Particle average sizes of fractions d_1, d_2, d_3 and d_4 were given in Table 2.1 above. Y-axis in Figure 2.9 shows the weight fraction of each particle size. Weight fraction of particles in binary particle systems (d_1-d_3, d_1-d_4, d_2-d_3, and d_2-d_4) were 0.5. For ternary beds (d_1-d_2-d_3 and d2-d3-d4) and mixed particle system (d_1-d_2-d_3-d_4) weight fraction of particles were 0.333 and 0.25, respectively.

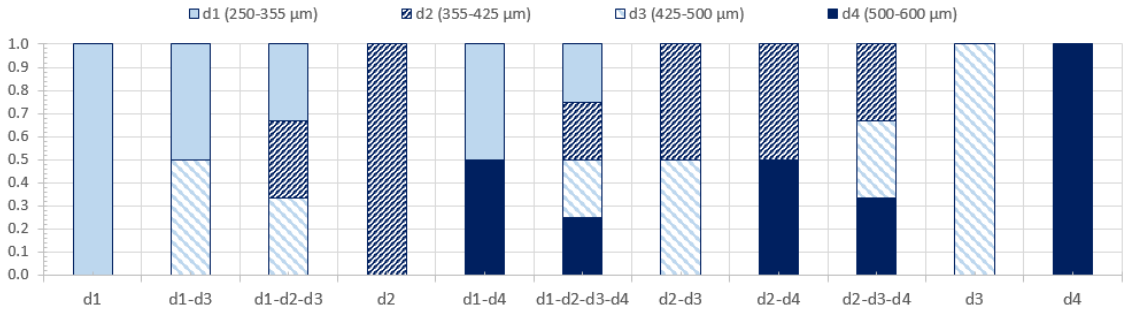

Figure 2.7. Eleven different particle bed compositions and their weight fractions used in this study.

2.6. Average Particle Size in Polydisperse Beds

The particle size in a polydisperse bed were characterized using two different formulas. Weight averaged particle size was defined with equation 2.1.

$$d_p = \frac{1}{\sum_i \frac{x_i}{d_{pi}}} \tag{2.1}$$

Where,

d_p = weight averaged particle size;

x_i = weight fraction of particle size d_{pi}

Other method calculates the average particle diameter employing arithmetic mean. An example of calculations is shown below for a binary bed composed of 25 g of d_1 and d_3 (Figure 2.8).

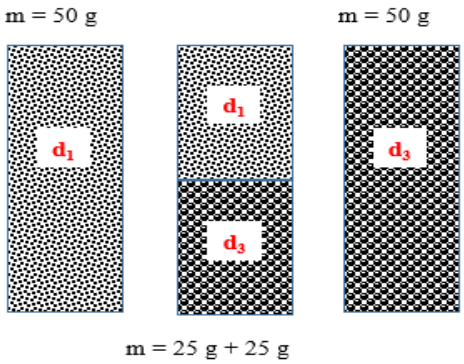

Weight average particle size of binary bed d_1-d_3: $d_p = \dfrac{1}{\dfrac{0.5}{d_1} + \dfrac{0.5}{d_3}} = 366\ \mu m$

Arithmetic average particle size of binary bed d_1-d_3: $d_p = \dfrac{d_1 + d_3}{2} = 383\ \mu m$

Figure 2.8. An example for calculation of average particle size of a polydisperse bed.

Average particle sizes for all particle compositions used in this study were calculated and is shown in Figure 2.9.

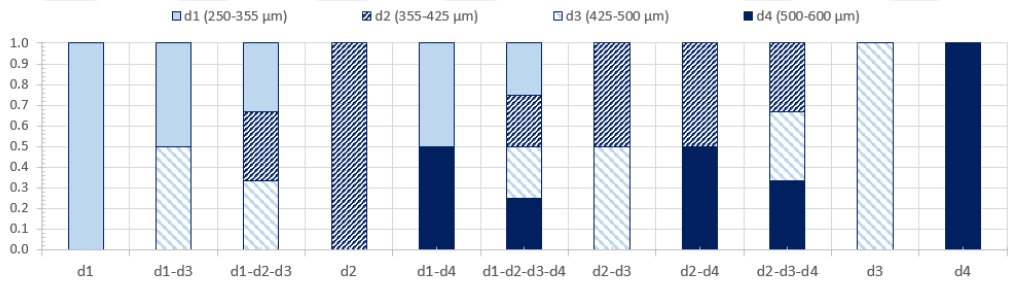

	d1	d1-d3	d1-d2-d3	d2	d1-d4	d1-d2-d3-d4	d2-d3	d2-d4	d2-d3-d4	d3	d4
weight averaged (µm)	303	366	374	390	390	406	423	456	459	463	550
arithmetic mean (µm)	303	383	385	390	426	426	426	470	468	463	550

Figure 2.9. Weight averaged and arithmetic mean average particle sizes of polydispersed beds.

2.7. Determination of Mass Transfer Coefficients

Experiments were performed to determine mass transfer coefficients of polydispersed beds used in the study. Same experimental column (21.9 mm ID and 100 cm height) was operated at the particle composition and at the same flowrate studied in fluidized bed ion exchange experiments. Only difference in operation was that the tank receives

the column effluent during the experiment. Samples were collected both from the column effluent and from the reservoir in every 5 minutes. Concentration profiles for reservoir and column effluent were drawn. Equation 2.2 was employed for the determination of mass transfer coefficients.

$$k_L = \frac{Q}{A} \ln \frac{C_{in}}{C_{out}}$$

(2.2)

Where,

k_L = mass transfer coefficient, cm/min

Q = volumetric flow rate, mL/min

A = total surface area of particles in the bed (cm^2)

C_{in} and C_{out} are the concentrations of ammonium ion ($mgNH_4^+/L$) in reservoir and column effluent, respectively (Figure 2.10).

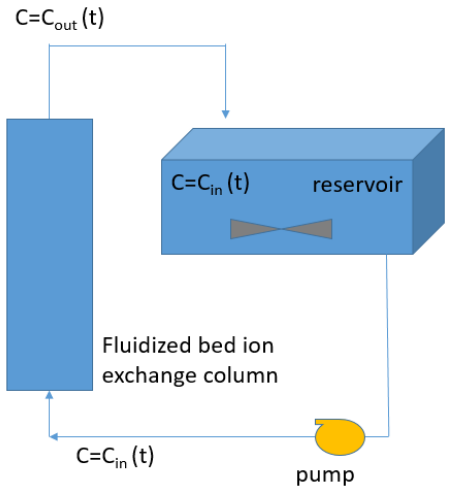

Figure 2.10. A schematic view of experiment employed in determination of mass transfer coefficient.

Procedure employed in calculation of total surface area of particles in the bed was explained in Section 2.9

2.8. Calculation of System Parameters and Performance Evaluation Tools

Volume of bed, fluidized bed porosity, bed expansion and empty bed contact time (EBCT), linear (superficial) velocity, and interstitial velocity (Figure 2.11) were calculated using equations given below:

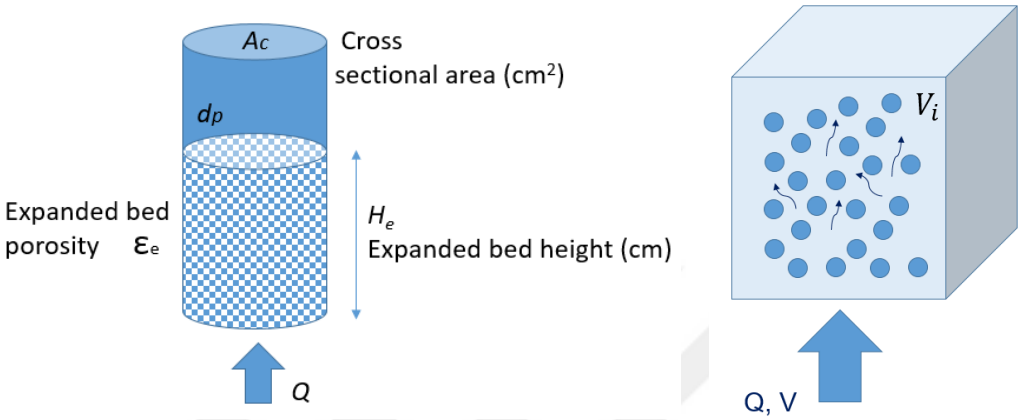

Figure 2.11. Representation of bed expansion, expanded bed porosity, linear velocity and interstitial velocity

Volume of expanded bed (Ve):

Volume of expanded bed is found by multiplying corss sectional area of the column (Ac) with the expanded bed height (He)

$$V_e = A_c \times H_e$$

(2..3)

Empty bed contact time (EBCT):

Empty bed contact time is the ratio between volume of expanded bed (Ve) and volumetric flow rate (Q)

$$EBCT = \frac{V_e}{Q} \qquad (2.4)$$

Linear (superficial) velocity (V):

Linear velocity is the ratio of volumetric flow rate (Q) to the cross sectional area of the

fluidization column (A_c)

$$V = \frac{Q}{A_c} \tag{2.5}$$

Intersititial velocity (V_i):

Interstitial velocity is the actual velocity of liquid within the pores and found by dividing linear velocity (V) to expanded bed porosity (ε_e).

$$V_i = \frac{V}{\varepsilon_e} \tag{2.6}$$

Expanded bed porosity (εe):

Expanded or fluidized bed porosity is calculated using the formula below:

$$\varepsilon_e = 1 - \frac{\frac{M}{\rho}}{V_e} \tag{2.7}$$

Where,

M: mass of clinoptilolite used in bed (g)

ρ: density of clinoptilolite (g/cm3). A particle density of clinoptilolite of 1.6 g/cm3 is used.

Ve: Volume of expanded bed (cm3)

Breakthrough Time (t_b):

Breakthrough point which is taken as the time when $C_{eff} = 0.10 \times C_0$

Exhaustion Time (t_x):

The exhaustion time is defined as the time of operation when $C_{eff} = C_0$

t_b and t_x were determined from the breakthrough curve. Breakthrough curve (Figure 2.12) is the plot which shows the variation in effluent concentration (C_{eff} or C) or relative concentration (C/C_0) with time.

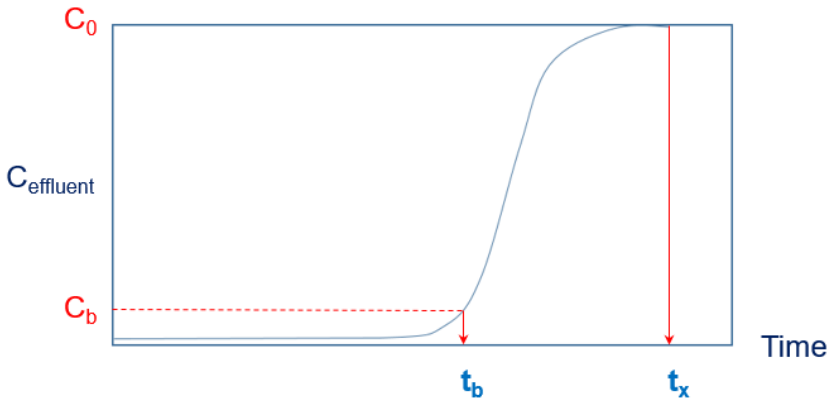

Figure 2.12. Breakthrough curve

Volume of water (L) passed through the column until the time of breakthrough (V_b) and volume of water (L) passed through the column during the entire run (V_x) were determined by multiplying flowrate (Q) with t_b and t_x, respectively.

Bed Volume (BV):

Bed volume (BV) is calculated for each sampling time (t) by dividing the volume of water passed through the fluidized bed to the volume of clinoptilolite bed including the pores (A_cH, H is the settled height or fixed bed height of the clinoptilolite in column). Volume of clinoptilolite bed was found by multiplying the cross sectional area of the column with the depth of medium.

$$BV = \frac{Q_t}{A_c \times H} \tag{2.8}$$

Ammonium Ion Loading:

Ammonium ion loading (mass of ion as mg NH_4^+) up to time of sampling (t in minutes) can be found by multiplying the rate of flow (Q in liters per minute) and ammonium ion concentration in feed flow (C_0 in mg NH_4^+/L) with that time (t) at which a sample from the effluent was collected. Dimensionless time scale at any time during an experiment can be found by dividing NH_4^+ loading at that certain time (QC_0t) to the cumulative NH_4^+ loading for bed exhaustion (QC_0t_f). Here t_x represents the time at which all exchange sites on clinoptilolite in fluidized bed are exhausted (effluent concentration is

being equal to influent concentration $C_{eff} = C_0$).

Breakthrough Capacity (*Br-Cp*) / Exhaustion Capacity (*Ex-Cp*):

Br-Cp / *Ex-Cp*

The term "breakthrough capacity / exhaustion capacity" is an indication of column efficiency. This ratio increases when the column is used efficiently It is calculated by dividing area above breakthrough curve until breakthrough time to the area over breakthrough curve until the exhaustion point (Figure 2.13).

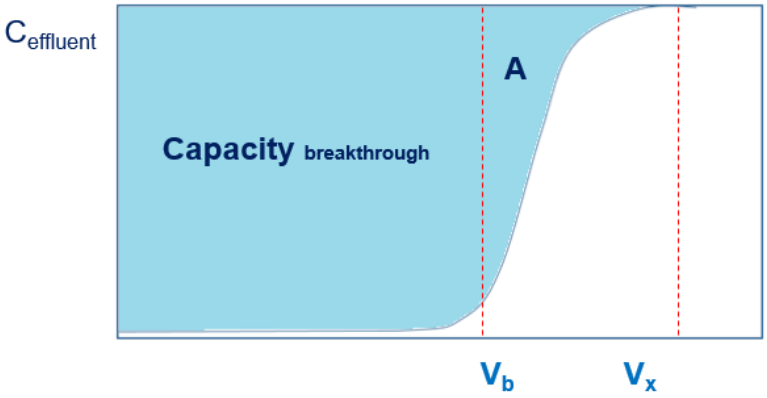

Figure 2.13. Breakthrough capacity and total (exhaustion) capacity.

Exhaustion (or total) capacity of the bed is the area shown as blue color in Figure 2.13 (the sum of breakthrough capacity and area A, the remaining capacity).

$$Breakthrough\ capacity = C_0 V_b - \int_0^{V_b} f(V,C)dV$$

$$Remaining\ capacity = C_0(V_x - V_b) - \int_{V_b}^{V_x} f(V,C)\,dV$$

Bed Usage Rate (BUR)

Bed usage rate was also calculated for each experiment. BUR shows the difference in concentration (feed water ammonium ion concentration minus the average effluent concentration up to breakthrough time) per uptake of ammonium by clinoptilolite (X/M in $mgNH_4^+$ per mass of clinoptilolite used) until the time of breakthrough. Average ammonium ion concentration calculation using the breakthrough curve is shown in Figure 2.14.

BUR has a unit of gram clinoptilolite (in which the exchage takes place during breakthrough) per liter of water treated in that period.

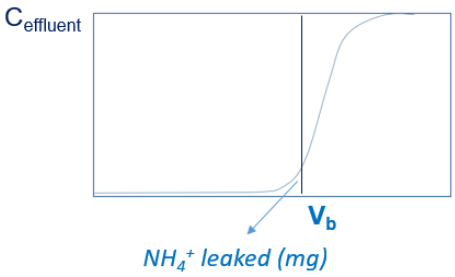

$$C_{1\_average} = \frac{NH_4^{+}\,(mg)}{V_b\,(L)}$$

Figure 2.14. Calculation of average ammonium ion concentration during breakthrough.

Bed Usage Rate (g clinoptilolite / L water) is calculated using the equation below:

$$BUR = \frac{C_0 - C_{1\_ave}}{(\frac{X}{M})_b} \qquad (2.7)$$

Fractional capacity (F):

Fractional capacity is the ratio of NH_4^+ exchange capacity of the bed remaining after breakthrough (area A in Figure 2.15) to NH_4^+ ion loading between time breakthrough and exhaustion time (sum of area A and B in Figure 2.15). F ratio decreases when the column is used efficiently.

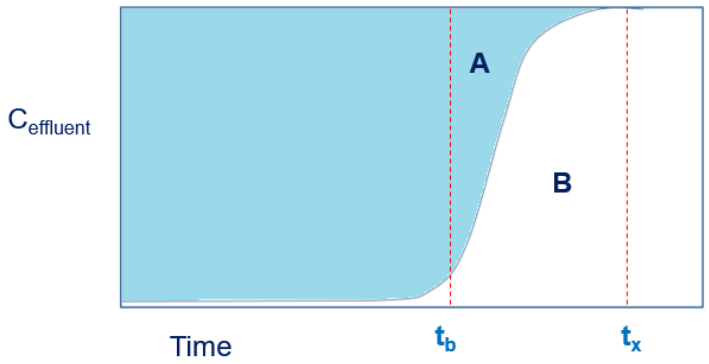

$$F = \frac{A}{A + B}$$

Figure 2.15. Calculation of fractional capacity

Fractional capacity ($mgNH_4^+/mgNH_4^+$) is calculated using the equation below:

$$F = \frac{(Ex\_Cp) - (Br\_Cp)}{(V_x - V_b) \times C_0} \quad (2.8)$$

Mechanical dispersion coefficient (K):

Mechanical dispersion is caused by the different flow paths of water travelling in a porous medium. Some of the flow paths are faster because they follow a more direct path. Other flow paths may be slower. K, the coefficient of mechanical dispersion (cm^2/min) in the liquid phase, is calculated by multiplying the interstitial velocity with a characteristic medium length taken as average particle size in the bed.

K = intersititial velocity × characteristic medium length

2.9. Overall particle surface area of the bed (A):

The surface area of each fluidized beds were calculated using the equation below:

$$A = V_e \times (1 - \varepsilon_e) \times \frac{6}{d_p} \quad (2.9)$$

Where,

A = surface area of granular system

V_e = expanded bed volume

ε_e = expanded bed porosity

d_p = weight average particle size

In course of this study weight averaged and arithmetic mean particle sizes of all the particles are calculated. These values are shown in Figure 2.10. The calculated weight averaged particle size values are using in the calculation of particle surface area of a

granular system.

The overall particle surface areas of mono and polydispersed particle systems were calculated and are shown in Figure 2.16.

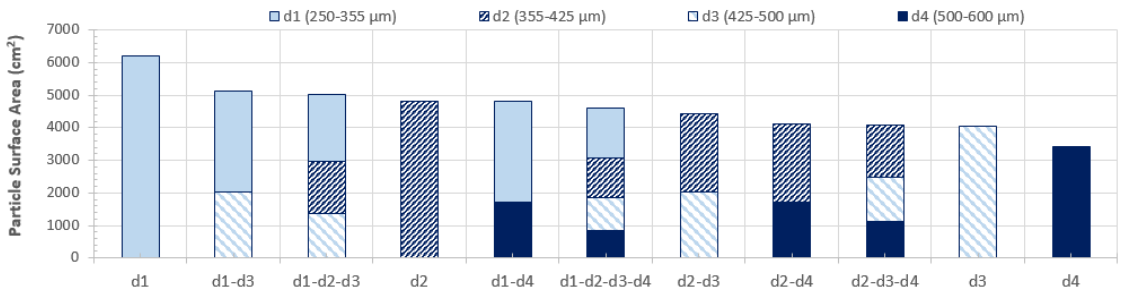

Figure 2.16. Overall particle surface areas for mono and poly

3.RESULTS AND DISCUSSION

Fluidized bed ion exhchange experiments were performed in columns to investigate the removal performance of ammonium ion. Particle size fractions used in these experiments were d_1 = 250-355 μm, d_2 = 355-425 μm, d_3 = 425-500 μm, and d_4 = 500-600 μm. Mass of clinoptilolite and ammonium ion concentration were constant and 50 g and 25 mg/L, respectively.

3.1. Fluidized Bed Experiments

Ion exchange of ammonium in fluidized beds of clinoptilolite was studied in following particle systems:

1) Monodispersed particle systems
2) Polydispersed particle systems

3.2. Monodispersed Particle Systems

Twenty two experiments were performed as monodispersed bed ion exchange experiments in which only one size of clinoptilolite was used. Four different size fractions of clinoptilolite were used: d_1 (250-355 μm), d_2 (355-425 μm), d_3 (425-500 μm) and d_4 (500-600 μm). All fluidized bed experiments with monodispersed particles were carried out at minimum of two different flow rates. Some experiments were conducted at a wide range of flow rate (bed expansion). The empty bed contact time in monodispersed fluidized bed experiments was ranged from 0.33 to 0.96 minutes. Operating conditions of fluidized bed ion exchange experiments performed on monodispersed beds were given in Table 3.1 – 3.4. These variables include flow rate, interstitial velocity, empty bed contact time, bed expansion, expanded bed porosity, temperature and ammonium ion concentration in feed solution.

Table 3.1. Fluidized bed ion exchange experiments using clinoptilolite with particle size fraction of d_1 (250-355 μm)

Flow rate (mL/min)	Interstitial velocity (cm/min)	Empty bed contact time (min)	Bed expansion ratio (%)	Expanded bed porosity	Temp. (^oC)	NH_4^+ conc. (mg/L)
75.8	35.16	0.96	56	0.572	19	23.2
97.1	40.94	0.87	81	0.63	19.5	24.6
119	45.68	0.85	117	0.692	21	24.1
242.9	80.89	0.63	230	0.797	20	25.15
244.7	80.54	0.66	246	0.807	21	32.25
248.7	81.41	0.66	254	0.811	20	25.05
290	94.2	0.59	266	0.817	20	25.3
320	101.49	0.6	310	0.837	20	24.4

Table 3.2. Fluidized bed ion exchange experiments using clinoptilolite with particle size fraction of d_2 (355-425 μm)

Flow rate (mL/min)	Interstitial velocity (cm/min)	Empty bed contact time (min)	Bed expansion ratio (%)	Expanded bed porosity	Temp. (^oC)	NH_4^+ conc. (mg/L)
100	49	0.68	50	0.54	20	25.3
200	75	0.54	138	0.709	17.5	24.4

Table 3.3. Fluidized bed ion exchange experiments using clinoptilolite with particle size fraction of d_3 (425-500 μm)

Flow rate (mL/min)	Interstitial velocity (cm/min)	Empty bed contact time (min)	Bed expansion ratio (%)	Expanded bed porosity	Temp. (^oC)	NH_4^+ conc. (mg/L)
100	50	0.67	25	0.531	17.5	24.8
200	86	0.4	51	0.614	18.3	24.6
290.3	113.39	0.34	114	0.68	20	27.5
384	133.73	0.34	188	0.762	20	25.15

Table 3.4. Fluidized bed ion exchange experiments using clinoptilolite with particle size fraction of d_4 (500-600 μm)

Flow rate (mL/min)	Interstitial velocity (cm/min)	Empty bed contact time (min)	Bed expansion ratio (%)	Expanded bed porosity	Temp. (^oC)	NH_4^+ conc. (mg/L)
75.967	43.39	0.77	32	0.465	19	26
97.6	51.8	0.64	42	0.5	19.5	24.4
110.2	59.58	0.56	39	0.491	20	24.1
119	49.54	0.72	96	0.638	21	25.2
290	115	0.33	115	0.669	20	25.65
407.7	141	0.33	205	0.768	20	25.35
409.1	141.25	0.33	207	0.769	21	25.2
456.4	151.99	0.34	250	0.797	20	25.5

Samples were taken from column effluents at 5-10 min time intervals. Feed water ammonium ion concentration was maintained constant and checked by taking samples at different durations of an experiment. Breakthrough curves were plotted after measuring all influent and effluent ammonium ion concentrations collected during the experiment. Three types of breakthrough curves were constructed. These are: i) variation in relative effluent concentration (C_{eff} / C_0) with time, ii) variation in relative effluent concentration (C_{eff} / C_0) with bed volume (BV), and iii) variation in relative effluent concentration (C_{eff} / C_0) with dimensionless time scale. Breakthrough point is selected as the point at which the concentration of ammonium ion in column effluent is equal to 10% of the influent concentration (C/C_0 = 0.10) as specified in Material and Methods section.

Fluidized bed ion exchange experiments conducted with using monodispersed particle size fractions of clinoptilolite were evaluated using the breakthrough curves plotted with the procedures explained above. Resulting graphs of all experiments were given in Appendix 3.

Breakthrough time, exhaustion time, breakthrough capacity, total capacity, ratio of breakthrough capacity to total capacity, bed usage rate, and fractional capacity values calculated for each fluidized bed ion exchange experiment with each particle size at different flow rates were given in Table 3.5 – 3.8.

Table 3.5. Results of fluidized bed ion exchange experiments using clinoptilolite with particle size fraction of d_1 (250-355 μm)

Exp.ID	Flowrate (mL/min)	t_b (min)	t_x (min)	BrCap ($mgNH_4^+$)	Tot Cap (mg NH_4^+)	BrCap /TotCap	F	BUR (g clino./L water)
d_1-1	75.8	409	820	698	1026	0.68	0.45	1.6
d_1-2	97.1	215	580	498	809	0.616	0.36	2.4
d_1-3	119	144	450	399	710	0.562	0.35	2.9
d_1-4	242.9	75	300	443	995	0.445	0.4	2.7
d_1-5	244.7	80	290	609	1175	0.518	0.34	2.6
d_1-6	248.7	72	295	428	811	0.528	0.28	2.8
d_1-7	290	60	310	413	878	0.471	0.25	2.9
d_1-8	320	22	225	163	657	0.249	0.31	7.1

Table 3.6. Results of fluidized bed ion exchange experiments using clinoptilolite with particle size fraction of d_2 (355-425 μm)

Exp. ID	Flowrate (mL/min)	t_b (min)	t_x (min)	BrCap ($mgNH_4^+$)	TotCap (mg NH_4^+)	BrCap /TotCap	F	BUR (g clino./L water)
d_2-1	100	75	317	178	1026	0.406	0.43	6.7
d_2-2	200	72	260	333	809	0.544	0.3	3.5

Table 3.7. Results of fluidized bed ion exchange experiments using clinoptilolite with particle size fraction of d_3 (425-500 μm)

Exp. ID	Flowrate (mL/min)	tb (min)	tx (min)	BrCap ($mgNH_4^+$)	TotCap (mg NH_4^+)	BrCap /TotCap	F	BUR (g clino./L water)
d_3-1	100	50	375	117	504	0.232	0.48	10
d_3-2	200	28	280	128	591	0.217	0.37	8.9
d_3-3	290.3	77	340	576	1267	0.454	0.33	2.2
d_3-4	384	12	320	107	1349	0.08	0.42	10.9

Table 3.8. Results of fluidized bed ion exchange experiments using clinoptilolite with particle size fraction of d_4 (500-600 μm)

Exp. ID	Flowrate (mL/min)	t_b (min)	t_x (min)	BrCap ($mgNH_4^+$)	TotCap (mg NH_4^+)	BrCap /TotCap	F	BUR (g clino./L water)
d_4-1	75.967	110	585	205	559	0.366	0.38	6
d_4-2	97.6	60	495	137	483	0.283	0.33	8.5
d_4-3	110.2	59	470	148	503	0.293	0.33	7.7
d_4-4	119	36	350	101	357	0.283	0.27	11.7
d_4-5	290	0	415	0	594	0	0.19	
d_4-6	407.7	0	265	0	1101	0	0.4	
d_4-7	409.1	0	285	0	1078	0	0.37	
d_4-8	456.4	0	225	0	1025	0	0.39	

Three types of breakthrough curves were constructed for monodisperse experiments. The breakthrough curves of the columns containing clinoptilolite particles in the size range of 250-355 µm are shown in Figures 3.1, 3.2 and 3.3. Three breakthrough curves are used in this section C_{eff}/C_0 with respect to time (min), C_{eff}/C_0 with respect to t/t_f and finally C_{eff}/C_0 against effluent volume passed through the column settled bed volume BV.

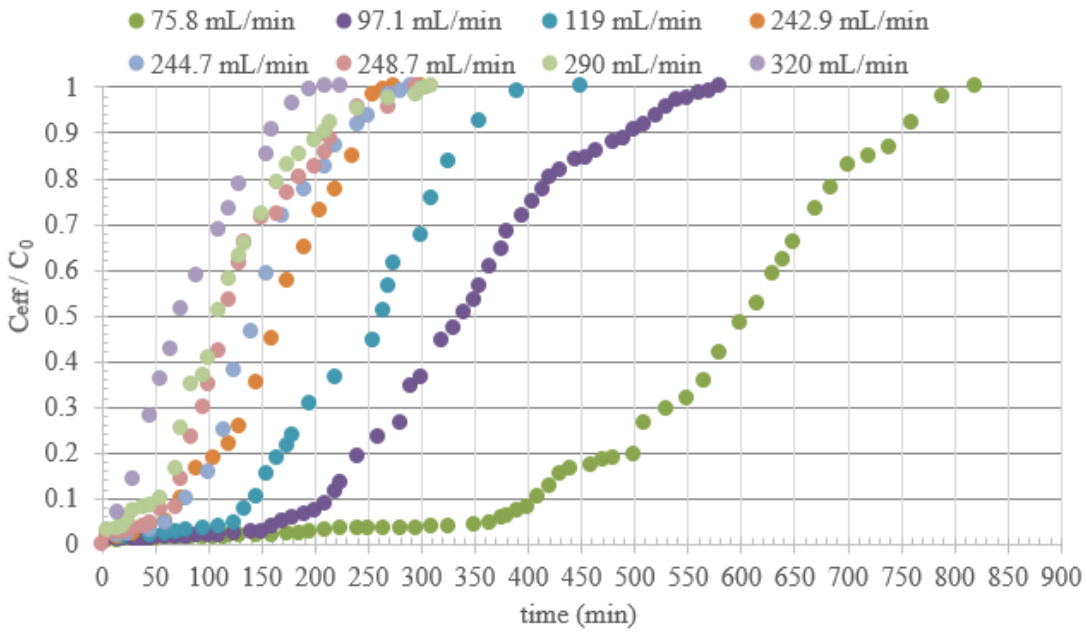

Figure 3.1. Variation in relative effluent concentration (C_{eff} / C_0) with time.

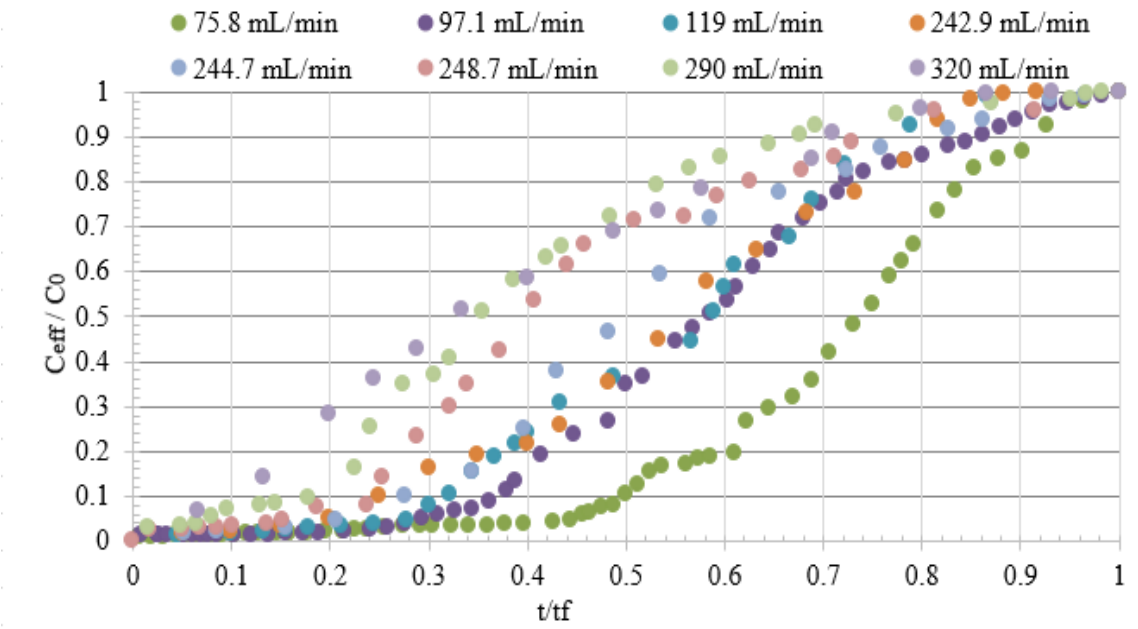

Figure 3.2. Variation in relative effluent concentration (C_{eff} / C_0) with dimensionless time scale.

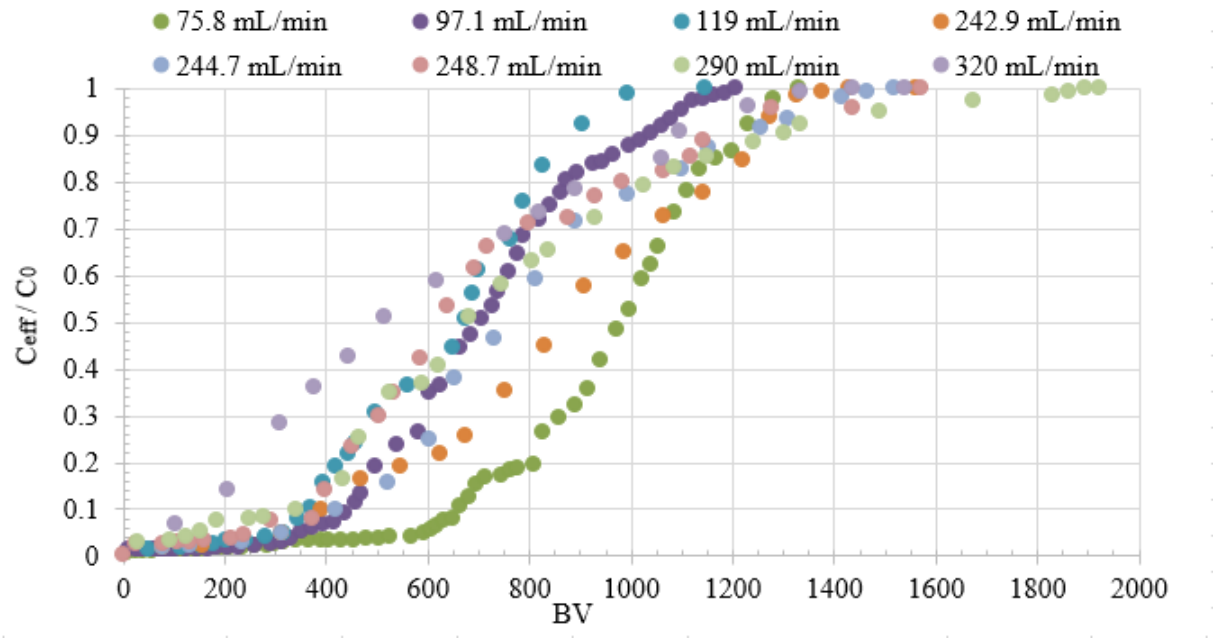

Figure 3.3. Variation in relative effluent concentration (C_{eff} / C_0) with BV.

The particles in size 250-355 µm performed well initially where voidage was in the range of 0.797 to 0.811 but the performance declined drastically with a further increase in the flow rate. It was seen that the shape of breakthrough curve shifts to the left with an increase in fluidization rate. Early breakthroughs were observed in fluidized beds operated at high flow rates. The breakthrough capacity/total capacity value ranged between 0.445 - 0.528 in the voidage range of 0.797 to 0.811 (see Table 3.1 and 3.5). As seen from Table 3.5 the exhaustion time decreases with increasing flow rate. Breakthrough capacity divided by total capacity was improved when the flow rates were increased to 242.9 - 244.7 and 248.7 mL/min. Bed usage rate parameters have also proved that improvement in performance (a decrease in bed usage rate implies a better performance as explained in Material and Methods section).

Three breakthrough curves were constructed for d_2 particle containing effluent ammonium concentration or C_{eff} (mg/l) with respect to time (min), C_{eff}/C_0 with respect to t/tf and finally C_{eff}/C_0 against effluent volume passed through the column settled bed volume BV. These curves are shown in Figure 3.4, 3.5 and 3.6.

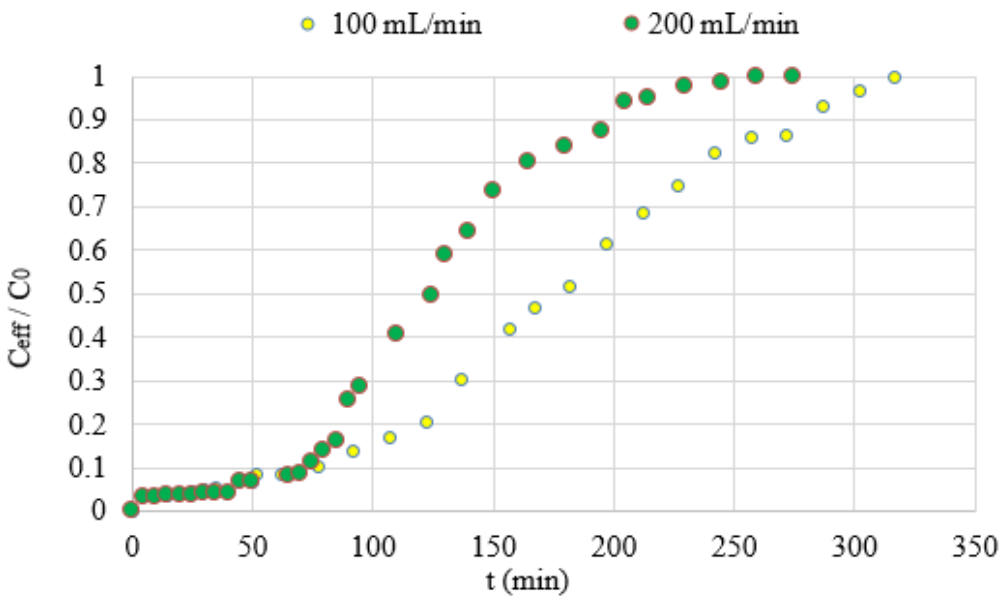

Figure 3.4. Variation in relative effluent concentration (C_{eff} / C_0) with time.

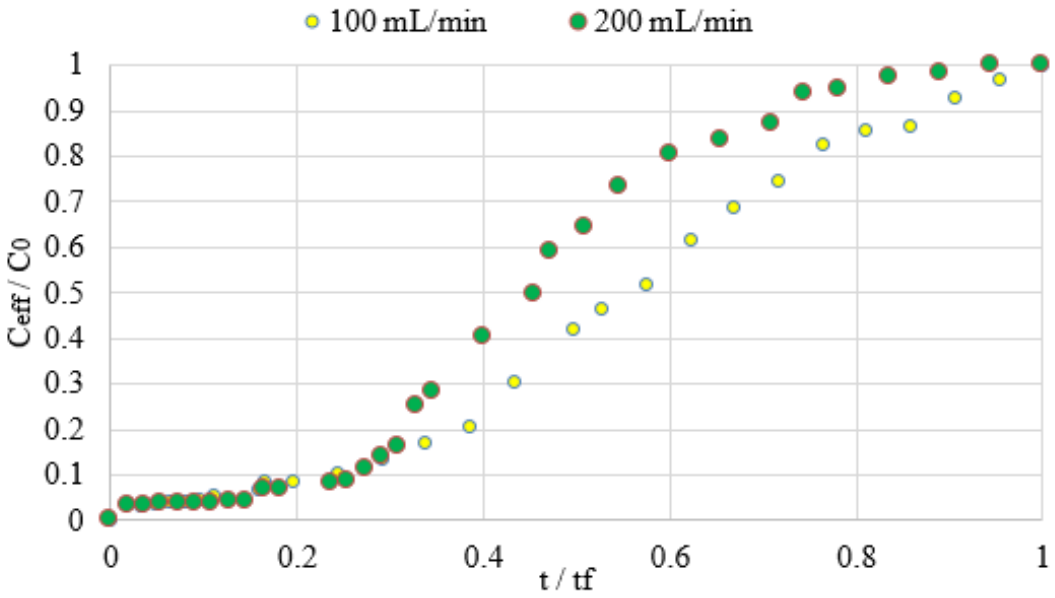

Figure 3.5. Variation in relative effluent concentration (C_{eff} / C_0) with dimensionless time scale.

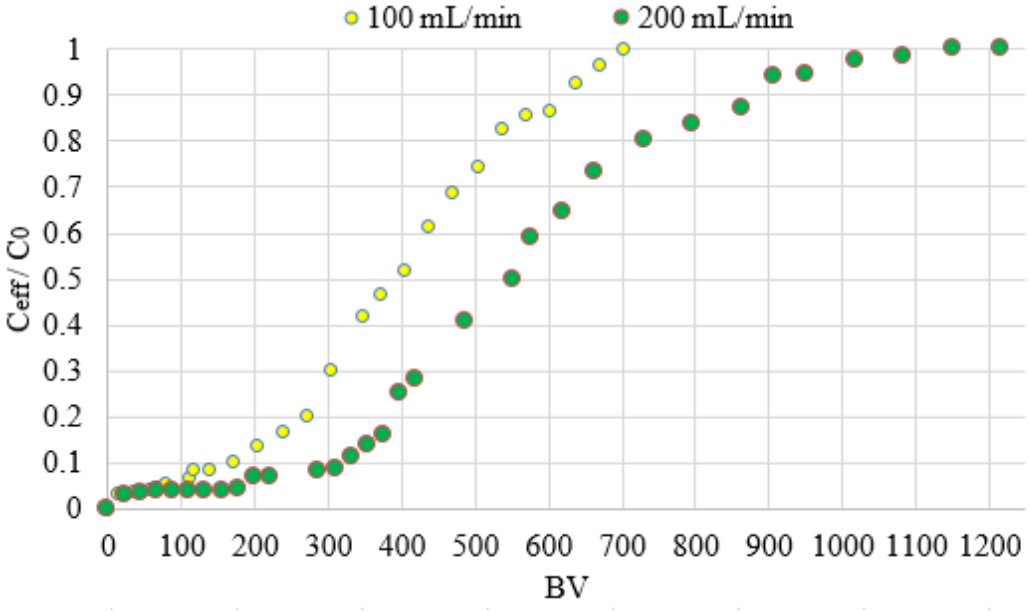

Figure 3.6. Variation in relative effluent concentration (C_{eff} / C_0) with BV.

The particles in size 355-425 µm performed well initially where voidage was not very high (0.54) but the performance declined with an increase in flow rate (at an expanded bed porosity of 0.709). An increase of breakthrough capacity / total capacity from 0.406

to 0.0.544 was observed (in Table 3.2 and 3.6). As seen from Table 3.6, the time needed for exhaustion decreases with increasing feed flow rate when the same amount and size of particles are used.

Three types of breakthrough curves were constructed for particle size d_3 are shown in Figure 3.7, 3.8 and 3.9.

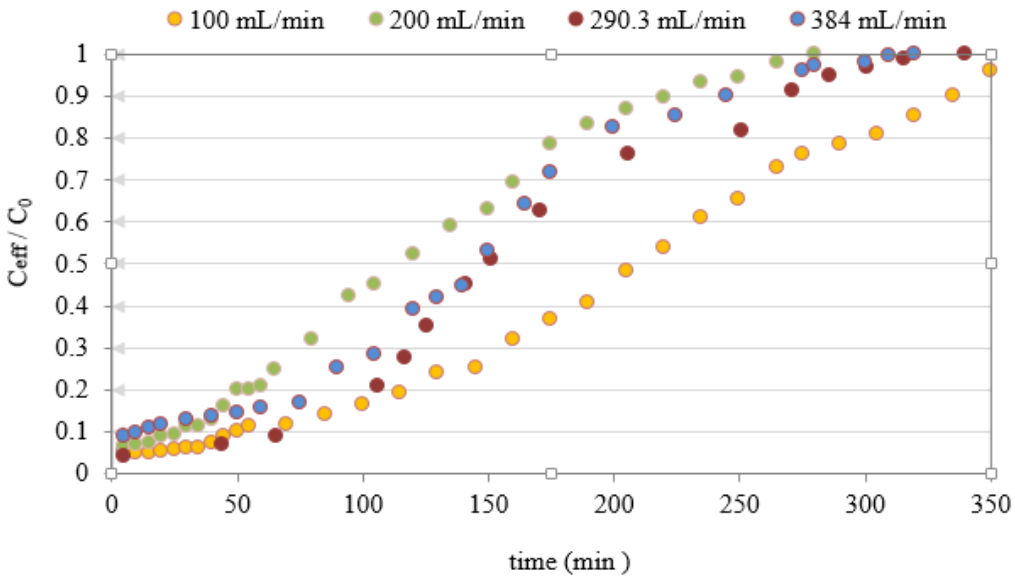

Figure 3.7. Variation in relative effluent concentration (C_{eff} / C_0) with time.

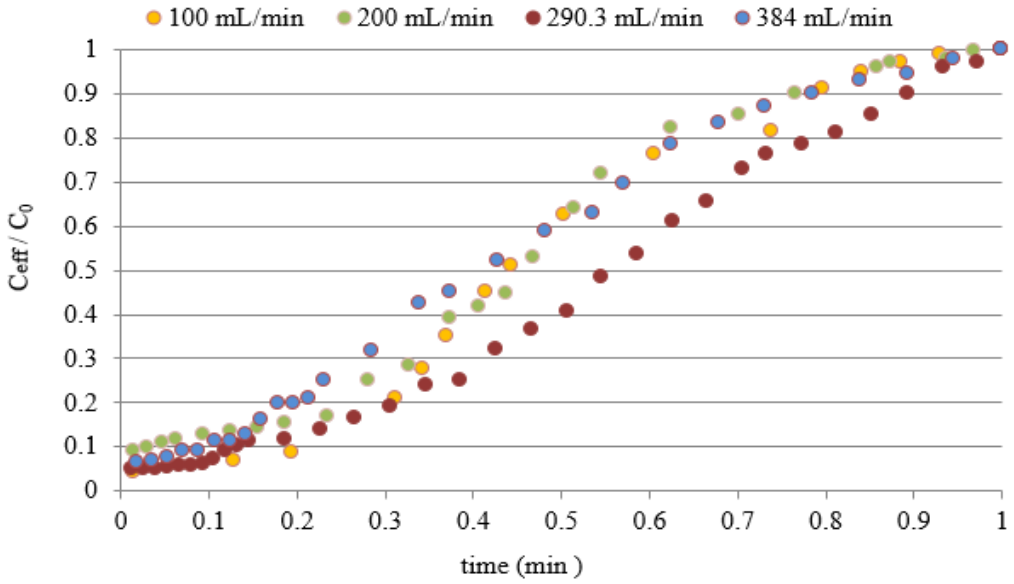

Figure 3.8. Variation in relative effluent concentration (Ceff / C0) with dimensionless time scale.

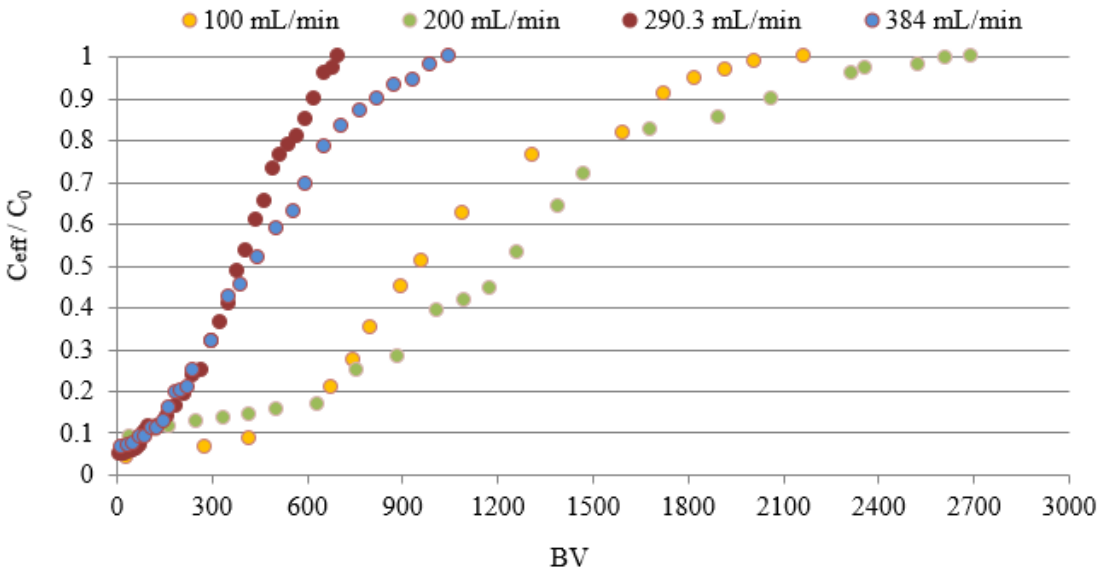

Figure 3.9. Variation in relative effluent concentration (C_{eff} / C_0) with BV.

Expanded bed porosity changed from 0.531 to 0.762 in fludized bed ion exchange studies conducted with 425-500 µm particle size monodisperse bed. Ratio of breakthrough capacity / total capacity was improved at a porosity of 0.68 (breakthrough capacity / total capacity = 0.454) compared to runs at expanded bed porosities of 0.531, 0.614 and 0.762 (see Table 3.3 and Table 3.7). An immediate leakage was observed in experiment performed at high fluidization rate (expanded bed porosity = 0.762).

The lowest performance of ion exchange of ammonium ion was observed in monodisperse experiments of particle size 500-600 µm. Immediate leakage was observed in those experiments (see Table 3.8 and Figure 3.10, 3.11, and 3.12).

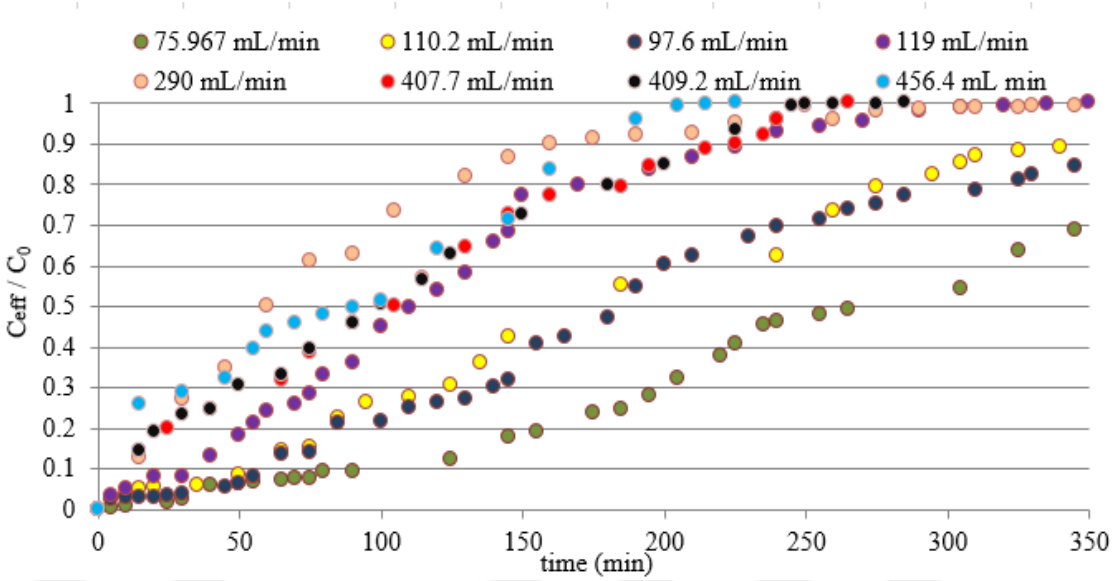

Figure 3.10. Variation in relative effluent concentration (C_{eff} / C_0) with time.

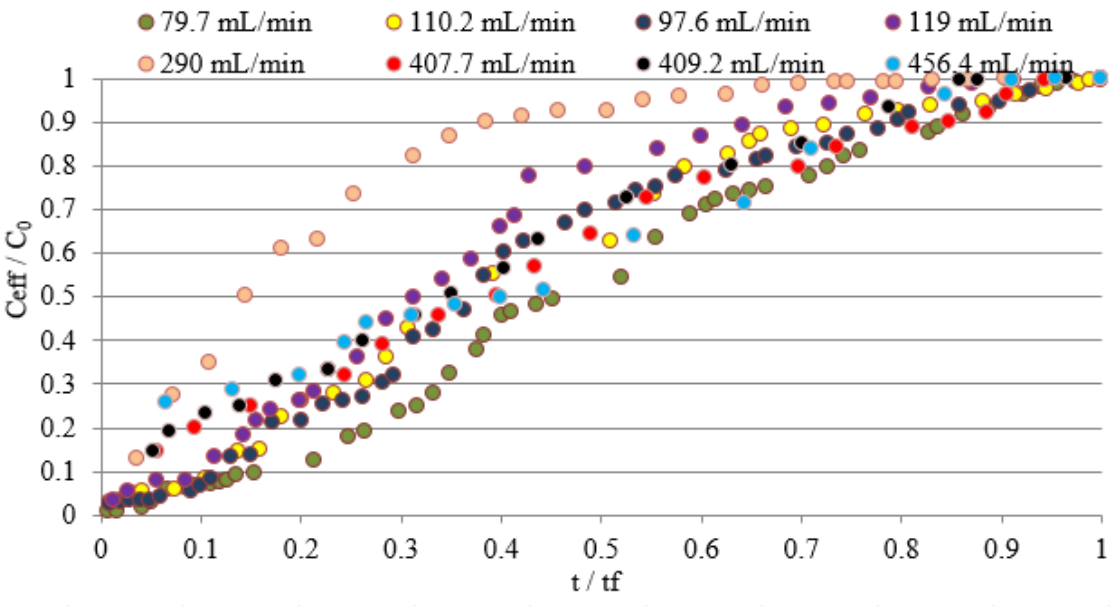

Figure 3.11. Variation in relative effluent concentration (Ceff / C0) with dimensionless time scale.

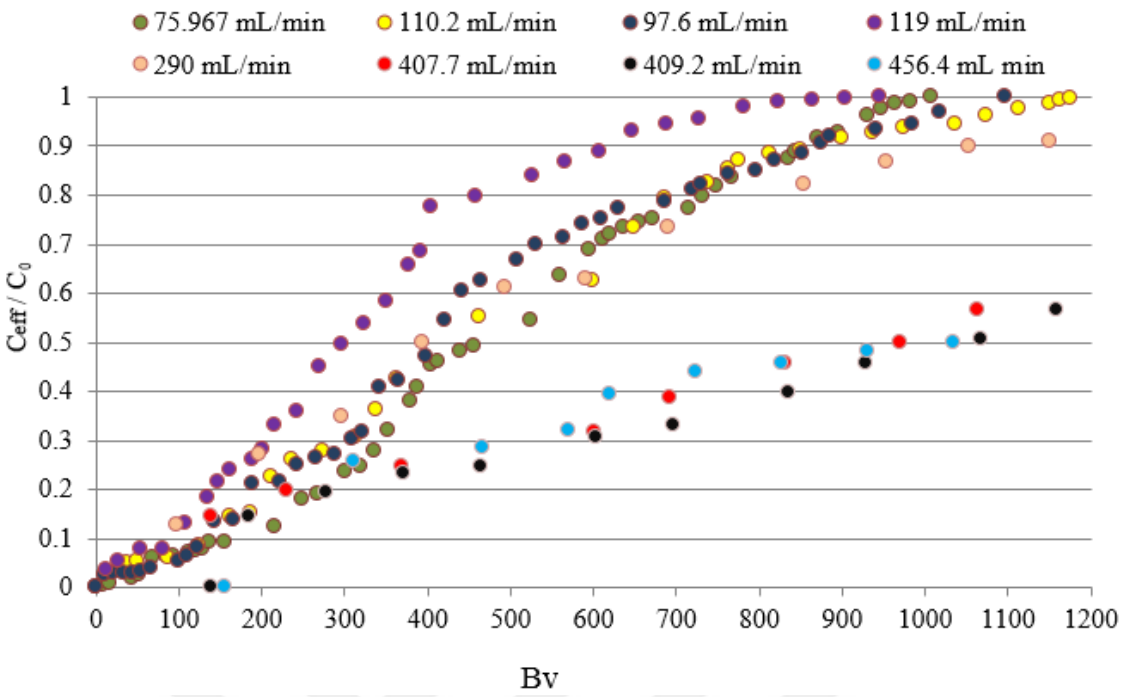

Figure 3.12. Variation in relative effluent concentration (C_{eff} / C_0) with BV.

Breakthrough times for all monodispersed particle systems operated at several different flow rates are included in Figure 3.13. Figure summarizes of the effects of both particle size and flow rate. Larger sized particles resulted in early breakthroughs. Shortened runs with early breakthroughs were also observed in experiments performed with finer particle sizes.

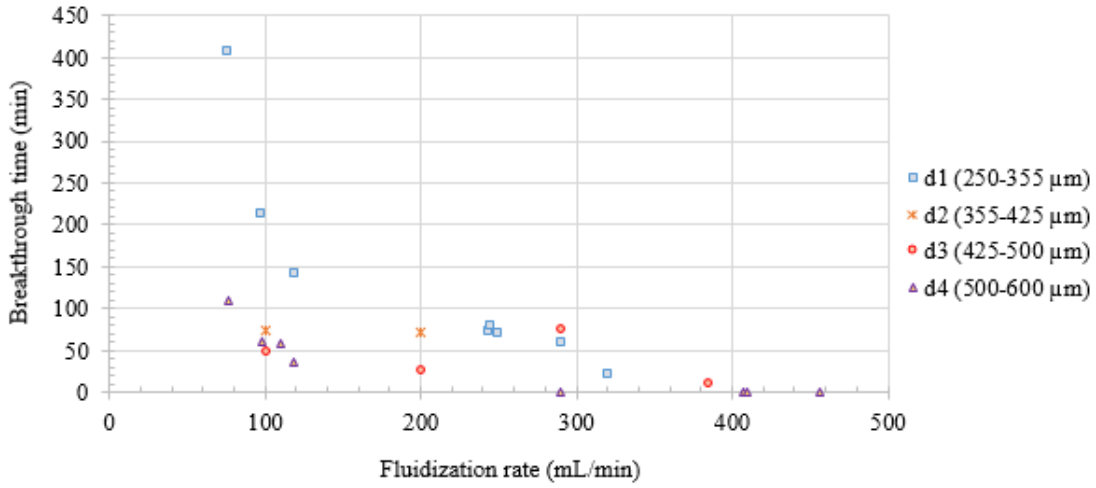

Figure 3.13. Variation in breakthrough time with fluidization rate

Same fluidization rate expands the finer composition bed at higher percentages As a result, change in fluidized bed porosity is different for each monosize bed composed of different particle size fraction. As seen from the figure, this is specifically observed in fine particle sizes (Figure 3.14). As it is evidenced in previous studies, a higher interstitial velocity and a low fluidized bed depth increases the mechanical dispersion of fluid within the pores and deteriorates the performance of the ion exchange bed.

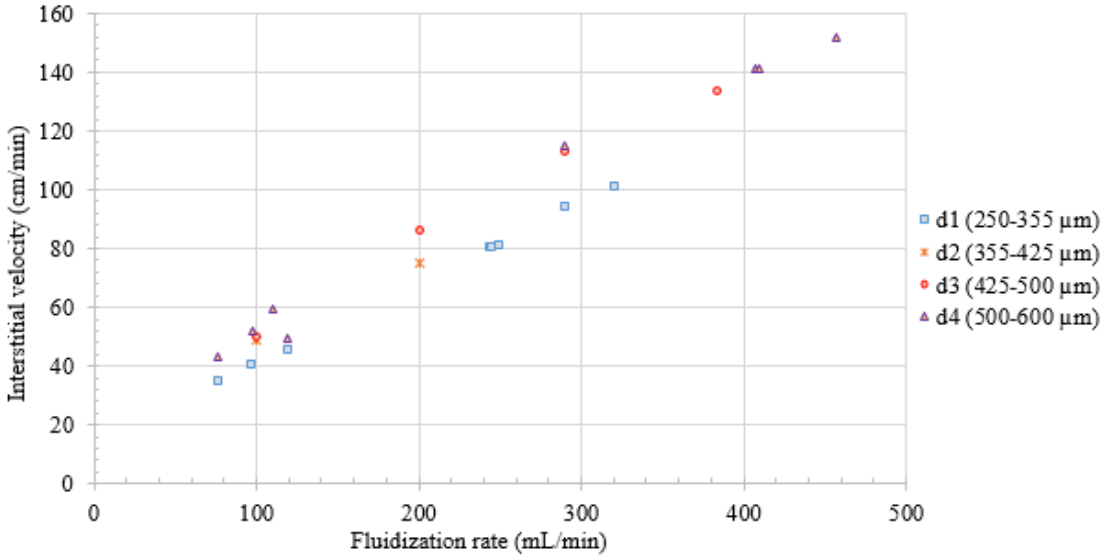

Figure 3.14. Variation in intersititial velocity with fluidization rate.

This is seen from Figure 3.15 which gives the breakthrough time of each monodisperse particle bed experiment at their interstitial velocity during operation. For larger sized particles early breakthroughs were observed than fine size particles at the same interstitial velocity. Decrease in breakthrough time was very sharp for fine sized particles. For coarser particles t_b values did not change much.

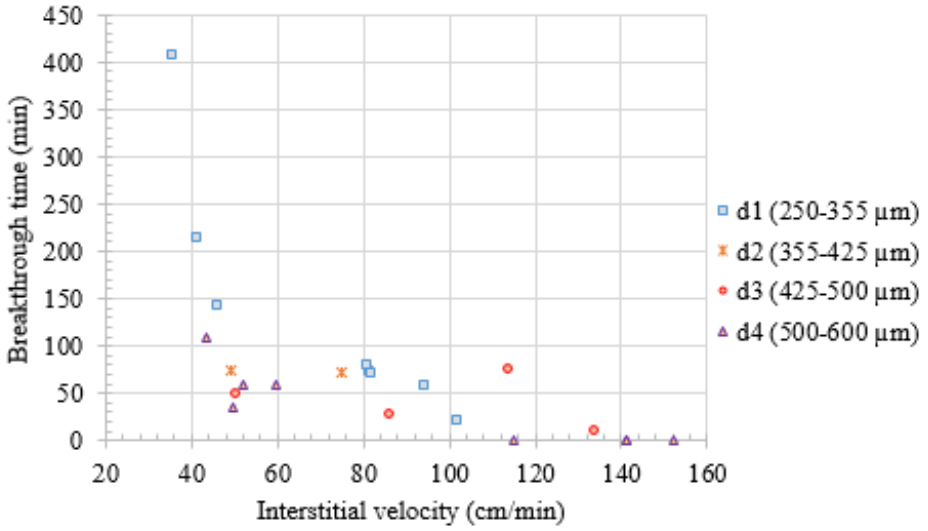

Figure 3.15. Variation in breakthrough time with intersititial velocity.

Bed exchange capacity at the time of breakthrough (breakthrough capacity) to the capacity at exhaustion (or total capacity) is a good indicator showing how efficiently the bed is used. Figure 3.16 includes the values of this ratio for all monodisperse fluidized bed experiments. After certain expanded bed porosity, this ratio dropped rapidly indicating the ammonium ion leakage just at the beginning of the experiment.

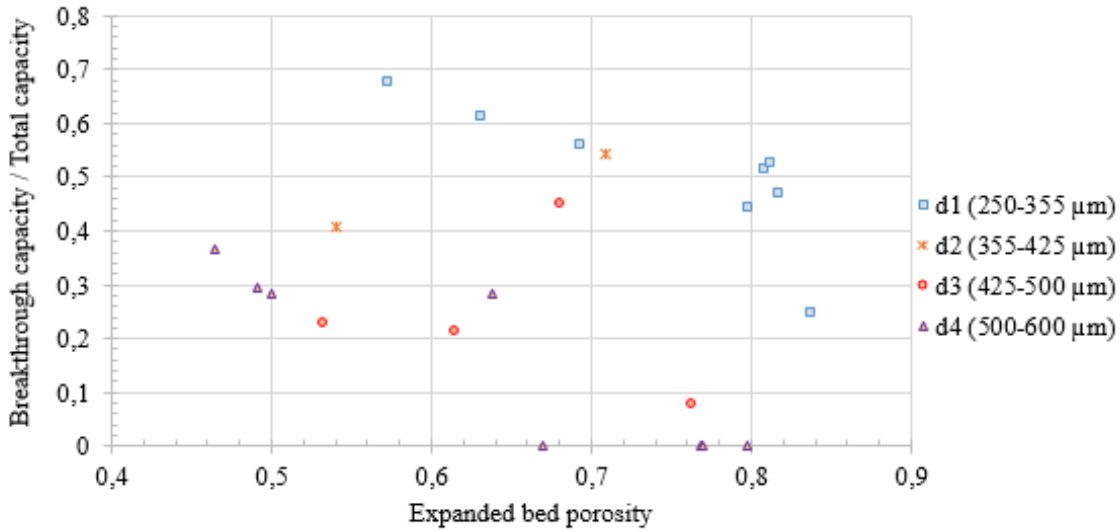

Figure 3.16. Variation in ratio of breakthrough capacity to total capacity versus expanded bed porosity.

Bed usage rate was also calculated for each experiment. BUR shows the difference in concentration (feed water ammonium ion concentration minus the average effluent concentration up to breakthrough time) per uptake of ammonium by clinoptilolite upto breakthrough time. Its unit is gram clinoptilolite in which the exchage takes place during breakthrough per liter of water treated in that period.

As seen from the Figure 3.17, value of this rate is low for monodisperse beds composed of fine size of particles. In other words, this type of fluidized beds uses the capacity of resin or ion exchange material slowly. When the particle size increases high values of bed usage rates were observed. Significant changes in bed usage rate were not observed for fine sized particles, whereas the increase in BUR was comparably high for largest particle size (500-600 µm).

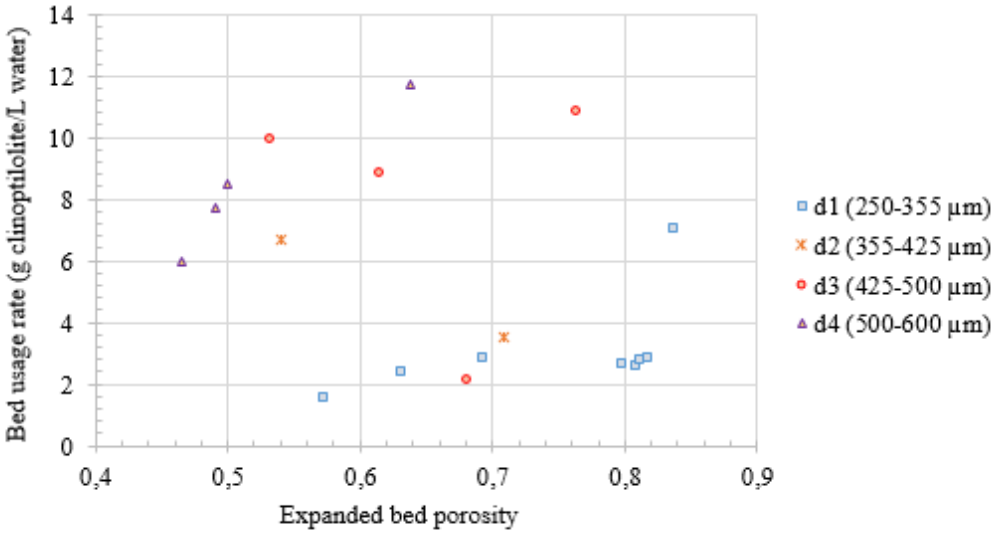

Figure 3.17. Variation in bed usage rate with expanded bed porosity

Two performance indicators used in comparisons (ratio of breakthrough capacity to total capacity and bed usage rate) were included in the two scales of Figure 3.18. For fine sized particles, except the experiment done at very high fluidization rate, resulted in low bed usage rates and a corresponding high breakthrough to total capacity ratio. For the experiments with d_2 and d_3 particle sizes, where the bed capacity is efficiently used it was seen that bed usage ratio is low and on the same order with fine sized particles.

For coarser particles, especially with at very fluidization rates, breakthrough capacity / total capacity ratios were very low with corresponding high bed usage rates.

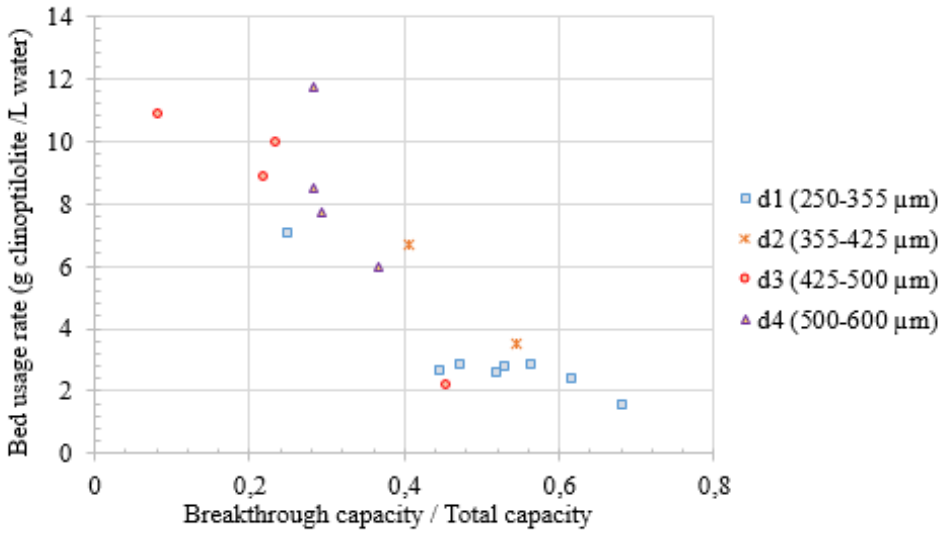

Figure 3.18. Variation in bed usage rate with breakthrough capacity / total capacity

3.3.Polydisperse Particle Systems

7 different compositions of particle mixtures were used in polydisperse beds (see Material and Methods section). Those are mixtures of d_1-d_3 (250-355 µm and 425-500 µm), d_1-d_2-d_3 (250-355 µm, 355-425 µm and 425-500 µm), d_1-d_4 (250-355 µm and 500-600 µm), d_1-d_2-d_3-d_4 (250-355 µm, 355-425 µm, 425-500 µm and 500-600 µm), d_2-d_3 (355-425 µm and 425-500 µm), d_2-d_4 (355-425 µm and 500-600 µm), d_2-d_3-d_4 (355-425 µm, 425-500 µm and 500-600 µm). All fluidized bed experiments with polydisperse particles were carried out at two different flowrates (100 and 200 mL/min). Mass of clinoptilolite used in these experiments was constant and 50 g for each particle size fraction.

Operating conditions of fluidized bed ion exchange experiments performed on polydispersed beds were given in Table 3.9 and Table 3.10. These variables include flow rate, interstitial velocity, empty bed contact time, bed expansion, expanded bed porosity, temperature and ammonium ion concentration in feed solution.

Breakthrough time, exhaustion time, breakthrough capacity, total capacity, ratio of breakthrough capacity to total capacity, bed usage rate, and fractional capacity values calculated for each fluidized bed ion exchange experiment with each particle size mixture at different two flow rates were given in Table 3.10 – 3.11.

Table 3.9. Fluidized bed ion exchange experiments of binary particle systems

Flow rate (mL/min)	Interstitial velocity (cm/min)	Empty bed contact time (min)	Bed expansion ratio (%)	Expanded bed porosity	Temp. (^oC)	NH_4^+ conc. (mg/L)
d_1-d_3-100	47	0.72	39	0.566	19	26
d_1-d_3-200	78	0.49	91	0.683	19.5	24.4
d_1-d_4-100	46	0.74	42	0.579	22.6	25.2
d_1-d_4-200	76	0.52	97	0.697	22.625	25.2
d_2-d_3-100	44	0.79	25	0.603	17.75	25.3
d_2-d_3-200	79	0.48	53	0.675	18.5	24.6
d_2-d_4-100	141.25	0.33	36	0.549	21.5	24.6
d_2-d_4-200	151.99	0.34	68	0.635	20	24.9

Table 3.10. Fluidized bed ion exchange experiments of polydisperse particle systems

Flow rate (mL/min)	Interstitial velocity (cm/min)	Empty bed contact time (min)	Bed expansion ratio (%)	Expanded bed porosity	Temp. (^oC)	NH_4^+ conc. (mg/L)
d_1-d_2-d_3-100	50	0.67	28	0.534	23.25	24.5
d_1-d_2-d_3-200	80	0.46	77	0.663	23	24.7
d_2-d_3-d_4-100	50	0.66	41	0.53	19.7	24.6
d_2-d_3-d_4-200	80	0.47	99	0.667	18.8	26.6
d_1-d_2-d_3-d_4-100	47	0.73	33	0.57	17	24.6
d_1-d_2-d_3-d_4-200	76	0.52	91	0.701	18	25.6
d_1-d_2-d_3-100	50	0.67	28	0.534	23.25	24.5
d_1-d_2-d_3-200	80	0.46	77	0.663	23	24.7

Table 3.11. Results of binary particle fluidized bed ion exchange experiments

Exp. ID	Flowrate (mL/min)	t_b (min)	t_x (min)	BrCap ($mgNH_4^+$)	TotCap (mg NH_4^+)	BrCap /TotCap	F	BUR (g clino./L water)
d_1-d_3-1	100	74	315	173	458	0.377	0.48	6.8
d_1-d_3-2	200	60	250	285	631	0.453	0.36	4.2
d_1-d_4-1	100	93	340	217	431	0.504	0.34	5.4
d_1-d_4-2	200	45	276	213	637	0.333	0.36	5.6
d_2-d_3-1	100	100	390	238	563	0.424	0.44	5
d_2-d_3-2	200	50.5	206	240	453	0.53	0.28	5
d_2-d_4-1	100	67	300	154	398	0.386	0.43	7.5
d_2-d_4-2	200	54	242	255	496	0.515	0.26	4.6

Table 3.12. Results of polydispersed particle fluidized bed ion exchange experiments

Exp. ID	Flowrate (mL/min)	t_b (min)	t_x (min)	BrCap ($mgNH_4^+$)	TotCap (mg NH_4^+)	BrCap /TotCap	F	BUR (g clino./L water)
d_1-d_2-d_3-1	100	63	402	144	550	0.261	0.5	7.9
d_1-d_2-d_3-2	200	48.3	215	225	487	0.461	0.32	5.2
d_2-d_3-d_4-1	100	68	370	157	456	0.345	0.4	7.4
d_2-d_3-d_4-2	200	67	215	338	604	0.561	0.34	3.7
d_1-d_2-d_3-d_4-1	100	152	482	353	793	0.445	0.54	3.3
d_1-d_2-d_3-d_4-2	200	53	233	256	521	0.492	0.29	4.7
d_1-d_2-d_3-1	100	63	402	144	550	0.261	0.5	7.9
d_1-d_2-d_3-2	200	48.3	215	225	487	0.461	0.32	5.2

Breakthrough curves of two polydisperse fluidized beds are included in Figure 3.19 (d_1-d_3 and d_1-d_2-d_3 fluidized ion exchange beds) because their total surface areas (5000 cm^2) are similar (see Material and Methods section). In the bed composed of d_1 and d_3 particle sizes, each with a mass of 25g, 60% of this total surface area is coming from d_1 particle size clinoptilolite and the rest 40% is coming from clinoptilolite with a particle size of d_3. On the other hand, in the bed composed of d_1 plus d_2 and d_3 particle sizes, each with a mass of 16.67 g, 41% of overall surface area is coming from d_1 particle size, which is the finest size in this study, and the remaining 32% and 27% surface area is because of d_2 and d_3 particle sizes, respectively.

The ratio of breakthrough capacity to total capacity was improved with increasing flow rate. Bed usage rate parameters have also proved that improvement in performance. Interstitial velocity and quantity representing mechanical dispersion were slightly higher in binary polydisperse bed than those calculated for ternary polydisperse bed.

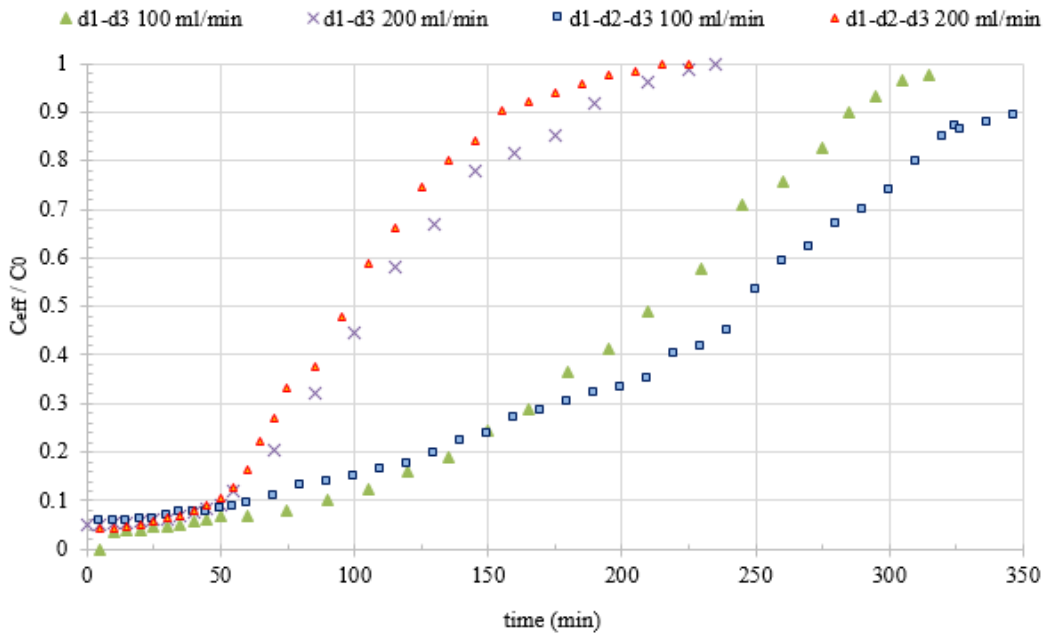

Figure 3.19. Variation in relative effluent concentration (C_{eff} / C_0) with time.

Table 3.13. Performance Summaries of polydisperse beds of d_1-d_3 and d_1-d_2-d_3

		d_1-d_3	**d_1-d_2-d_3**
Breakthrough Capacity / Total Capacity	100 mL/min	0.377	0.261
	200 mL/min	0.453	0.461
Intersititial Velocity	100 mL/min	47	50
(m/sec)	200	78	80
mL/min			
Bed Usage Rate	100	6.8	7.9
mL/min		4.2	5.2
(g clinoptilolite /L water)	200		
mL/min			
Fractional Capacity	100 mL/min	0.48	0.49
	200 mL/min	0.36	0.32
Empty Bed Contact Time	100 mL/min	0.72	0.67
(min)	200	0.49	0.46
mL/min			
Mass transfer coefficient	100		
mL/min		0.1157	
(cm/min)	200		
mL/min			
Mechanical dispersion coefficient	100	1.72	1.87
mL/min		2.85	2.99
(cm^2/min)	200		
mL/min			

Figure 3.20 shows three different types of fluidized bed: A monodisperse particle bed (with a particle size fraction of d_3), a binary bed 50% and 50% combinations in weight of d_2 and d_4 sizes, and a ternary bed consisting of d_2, d_3 and d_4 particle sizes. Overall surface area resulting from individual particles of different fractions in those beds is about same in these three beds (see Figure 2.12) and equal to approximately 4100 cm^2.

For 100 mL/min flow rate, d_2-d_4 and d_2-d_3-d_4 beds had an empty bed contact time of 0.33 and 0.66 minutes, respectively. Fluid velocity within the pores of d_2-d_3-d_4, (interstitial velocity) was higher compared to the bed composed of d_2-d_3 and d_4 mixture. Ratio of breakthrough capacity to total capacity for d_2-d_3-d_4 was slightly lower than d_2-d_4. The monosize bed of d_3 had the highest BUR in experiment 100 mL/min. Short contact times observed as in ternary bed as well as less expansion due to coarse particle sizes explain the lowest breakthrough performance. Breakthrough time was 50 min for this experiment. Highest BUR was obtained for this monosize particle bed (see Table 3.14) which shows that the available exchange sites were quickly expended during breakthrough. For 200 mL/min flow rate, ternary bed was showed the best performance. It has the lowest interstitial velocity and highest empty bed contact time among all three beds. Monosize bed, having the highest interstitial velocity and mechanical dispersion coefficient performed as the poorest. The earliest breakthrough was observed with this bed. These effects are also confirmed with the calculated values for fractional capacity of all set of experiments. Flow through experiments were carried out to calculate mass transfer coefficient (see Material and Methods section). Binary and ternary mixed beds had similar mass transfer coefficients which is also consistent with their ammonium exchange performance expressed as the ratio of breakthrough capacity to total capacity.

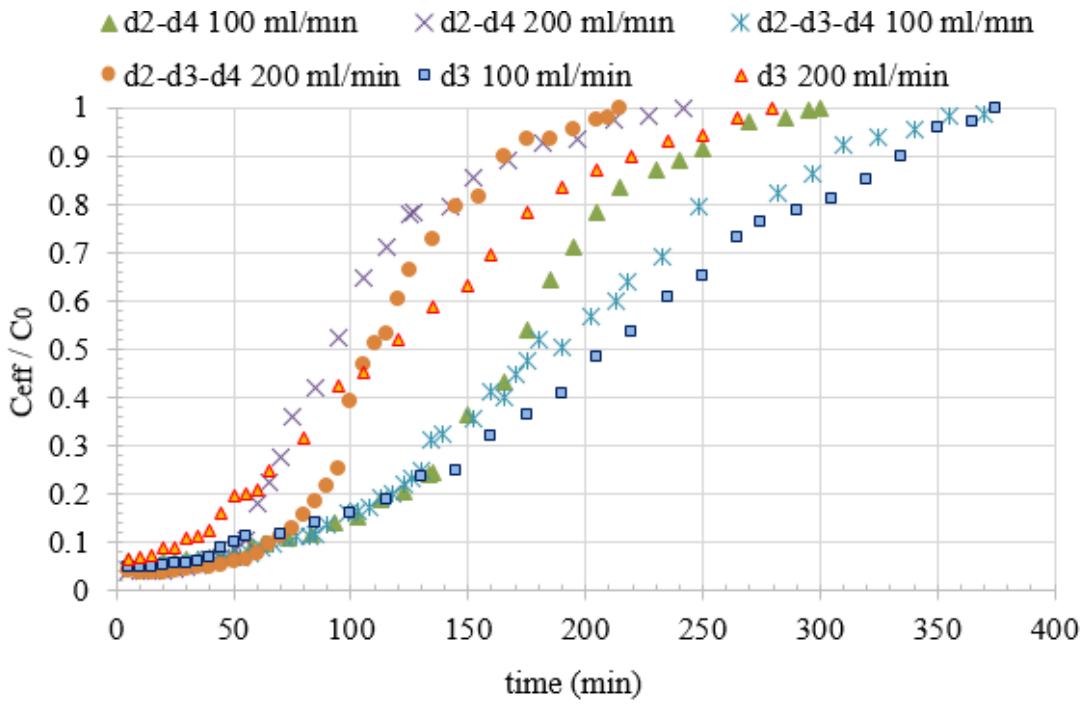

Figure 3.20. Variation in relative effluent concentration (C_{eff} / C_0) with time for d_2-d_4 and d_3 and d_2-d_3-d_4

Table 3.14. Performance Summaries of polydisperse beds of d_2-d_4, d_3 and d_2- d_3-d_4

		d_2-d_4	**d_3**	**d_2-d_3-d_4**
Breakthrough Capacity / Total Capacity	100 mL/min	0.386	0.232	0.345
	200 mL/min	0.515	0.217	0.561
Intersititial Velocity	100	48	50	50
mL/min		84	86	80
(m/sec)	200			
mL/min				
Bed Usage Rate	100	7.5	10	7.4
mL/min		4.6	8.9	3.7
(g clinoptilolite/L water)	200			
mL/min				
Fractional Capacity	100	0.43	0.48	0.4
mL/min		0.26	0.37	0.34
	200 mL/min			
Empty Bed Contact Time	100	0.69	0.67	0.66
mL/min		0.43	0.4	0.47
(min)	200			
mL/min				
Mass transfer coefficient	100	0.072		0.0729
mL/min		0.129		0.128
(cm/min)	200			
mL/min				

Mechanical dispersion coefficient	100	2.19	2.32	2.30
mL/min		3.83	3.98	3.67
(cm^2/min)	200			
mL/min				

Another comparison was made on a binary particle size bed and a monodisperse particle size bed. Average particle size of the binary was exactly the same of monodisperse particle bed. These are fluidized bed ion exchange column composed of uniform size range of d_2 and the binary particle size bed consisting of d_1-d_4 (finest and largest size particles used in this study) at same weight ratios. Experiments at 100 mL/min flow rate showed that binary particle size bed produced better breakthrough performance (an earlier breakthrough was observed in monodisperse bed). This was also seen from the BUR values of two columns (see Table 3.15). Doubling the flow rate from 100 mL/ min to 200 mL/min resulted in a decrease in bed performance for polydisperse bed. As seen from the Table 3.15, interstitial velocity and quantity representing mechanical dispersion were slightly higher in polydisperse bed than those calculated for monodisperse bed. Decrease in contact time because of high expansion ratio in binary bed was quite high (from 0.74 min to 0.52 min or from 44 seconds to 31 seconds).

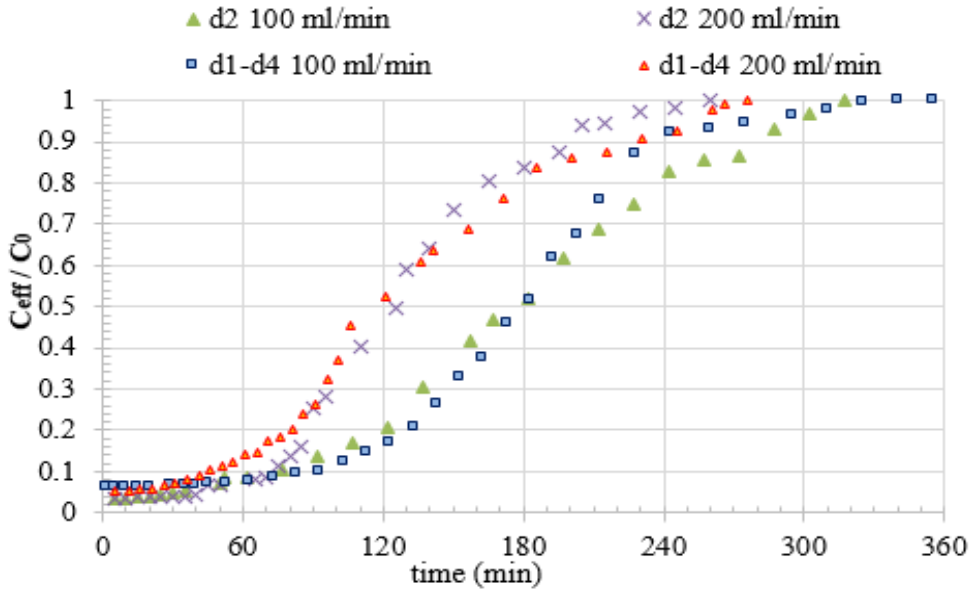

Figure 3.21. Variation in relative effluent concentration (C_{eff} / C_0) with time for d_2 and d_1-d_4

Table 3.15. Performance Summaries of polydisperse beds of d_2 and d_1-d_4

		d_2	d_1-d_4
Breakthrough Capacity / Total Capacity	100 mL/min	0.406	0.504
	200 mL/min	0.544	0.333
Intersititial Velocity (m/sec)	100 mL/min	49	46
	200 mL/min	75	76
Bed Usage Rate (g clinoptilolite/L water)	100 mL/min	6.7	5.4
	200 mL/min	3.5	5.6
Fractional Capacity	100 mL/min	0.43	0.34
	200 mL/min	0.3	0.36
Empty Bed Contact Time (min)	100 mL/min	0.73	0.74
	200 mL/min	0.52	0.52
Mass transfer coefficient (cm/min)	100 mL/min		
	200 mL/min	0.1121	
Mechanical dispersion coefficient (cm^2/min)	100 mL/min	1.91	1.79
	200 mL/min	2.93	2.96

Figure 3.22 shows the comparison of breakthrough curves of a binary bed (composed of d_2 and d_3 particle sizes) and a polydisperse particle bed consisting all four different size ranges of particles used in this study. Same column experiments were repeated at the same flow rates to measure mass transfer coefficients in these experiments. Values found from those experiments were consistent with the results obtained from breakthrough curve evaluations. As shown in Table 3.16 when the flow rate was doubled from 100 mL/min to 200 mL/min, the ratio of breakthrough capacity to total capacity improved. This was also seen from the values of mass transfer coefficients. Combinations of particle sizes with a high mass transfer coefficient, produced high breakthrough capacity to total capacites. Higher values of overall mass transfer coefficient was also observed for ion exchange experiments conducted at a high flow rate.

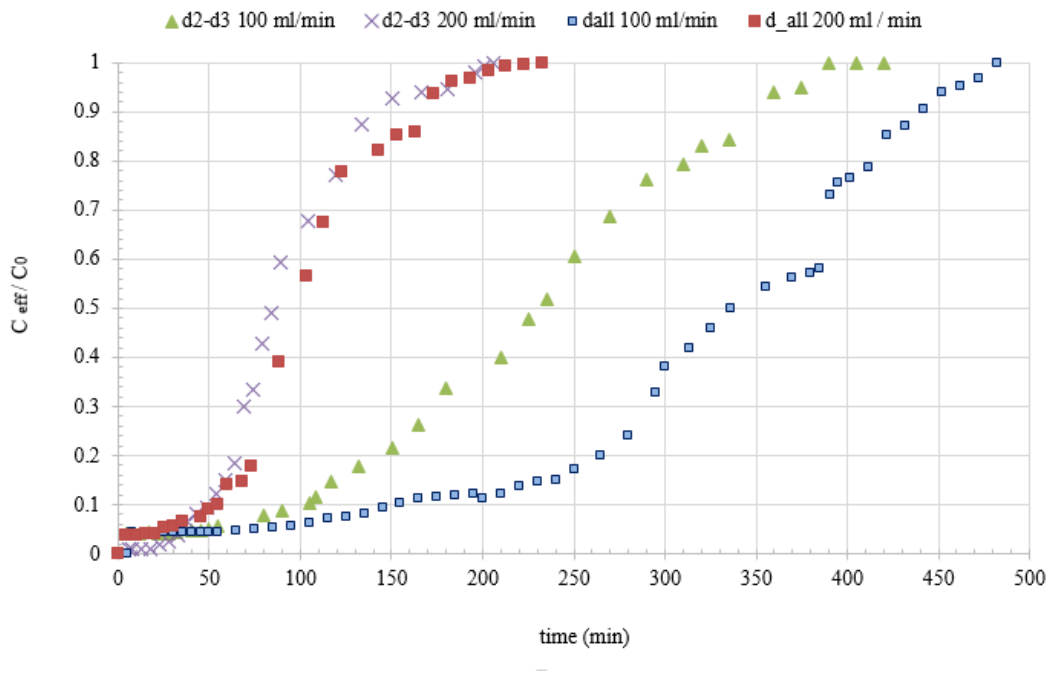

Figure 3.22. Variation in relative effluent concentration (C_{eff} / C_0) with time for d_2-d_3 and d_1-d_2-d_3-d_4

Table 3.16. Performance Summaries of polydisperse beds of d_2-d_4 and d_{all}

		$\mathbf{d_2 - d_3}$	$\mathbf{d_{all}}$
Breakthrough Capacity / Total Capacity	100	0.424	0.445
mL/min		0.53	0.492
	200		
mL/min			
Intersititial Velocity	100	44	47
mL/min		79	76
(m/sec)	200		
mL/min			
Bed Usage Rate	100	5	3.3
mL/min		5	4.7
(g clinoptilolite/L water)	200		
mL/min			
Fractional Capacity	100	0.44	0.54
mL/min		0.28	0.29
	200		
mL/min			
Empty Bed Contact Time	100	0.79	0.73
mL/min		0.48	0.53
(min)	200		
mL/min			
Mass transfer coefficient	100	0.0653	0.0455
mL/min		0.1392	0.1164
(cm/min)	200		
mL/min			
Mechanical dispersion coefficient	100	1.86	1.91
mL/min		3.34	3.09
(cm^2/min)	200		
mL/min			

Figure 3.23 shows all of the results of fluidized bed ion exchange columns composed of polydisperse particle mixtures. Experiments were grouped with respect to their flow rates. Higher flowrates producing a wider range of bed expansions (since the mixtures contain finer and coarser particles together) resulted in higher breakthrough capacity to total capacity ratios, the ratio used as a measure of bed performance.

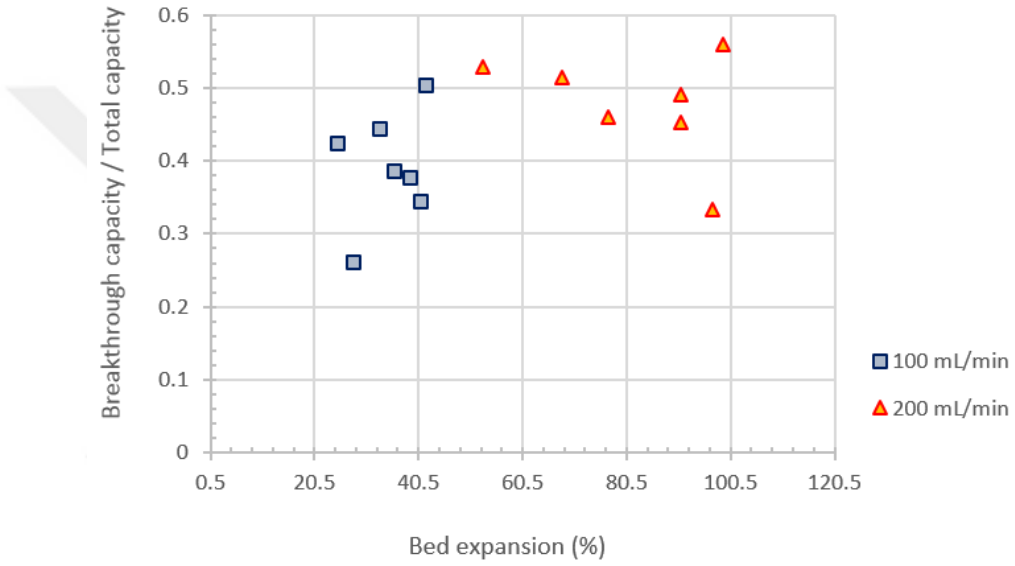

Figure 3.23. Change in ratio of breakthrough capacity to total capacity with bed expansion for all polydisperse beds studied

As explained before, for the experimental runs in which another set of experiment at the same flow rate and at the same particle composition were conducted, overall mass transfer coefficients were calculated and displayed in Figure 3.24. Figure displays the correlation between overall mass transfer coefficient and the performance indicator used (the ratio of breakthrough capacity to total capacity). Higher values of mass transfer coefficient were achieved for higher fluidization rates (bed expansions and porosities).

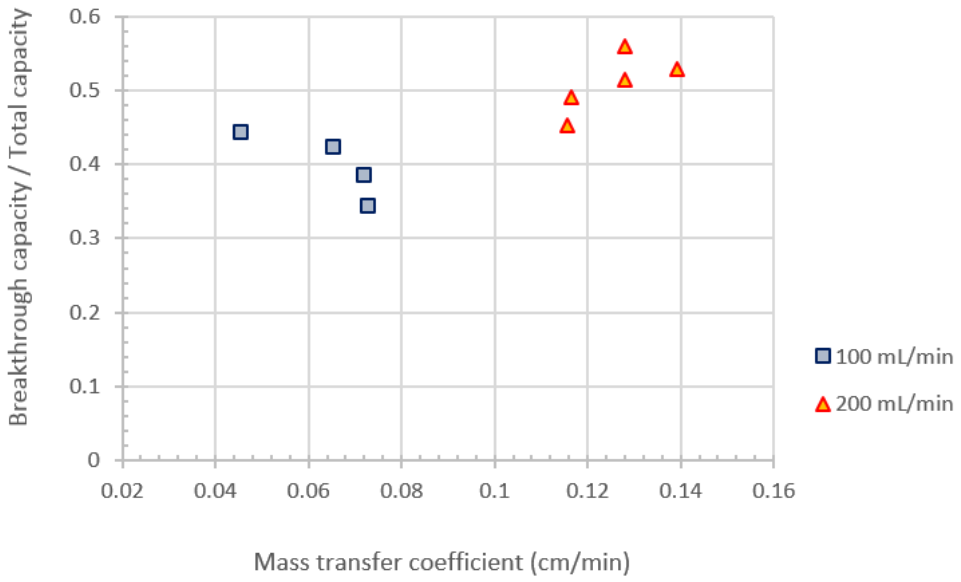

Figure 3.24. Correlation between mass transfer coefficient and ratio of breakthrough capacity to total capacity.

Effect of increase in bed porosity for experiments conducted at a higher flow rate on fractional capacity is given in Figure 3.25. Fractional capacity is the ratio of NH_4^+ exchange capacity of the bed remaining after breakthrough to NH_4^+ ion loading between time breakthrough and exhaustion time (see Material and Methods section). A breakthrough curve with a lower value of F represents the better performance of that particle mixture than the others with higher F values.

As seen from the Figure 3.25, increase in fluidized bed porosity decreases the F values of polydisperse beds.

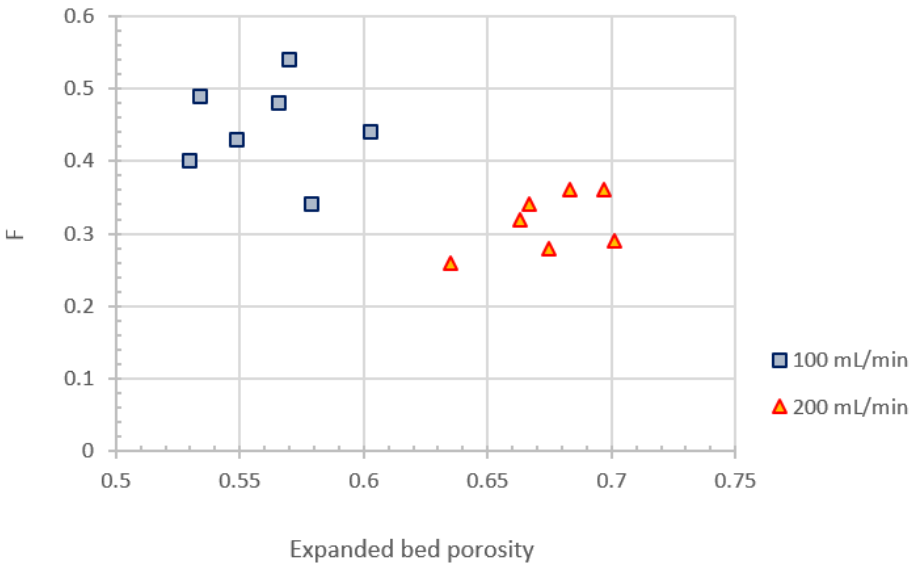

Figure 3.25. Variation in fractional capacity with expanded bed porosity in polydisperse beds.

Effect of increase in bed porosity on bed usage rate is shown in Figure 3.26. Bed usage rate (with a unit of mass of clinoptilolite per liter of water) expresses how quickly the bed expends the available exhchange sites during breakthrough (see Material and Methods section). As seen from the Figure 3.26, increase in flow rate, with fluidization, resulted in a decrease in bed usage rates, which is an indicator of a better performance.

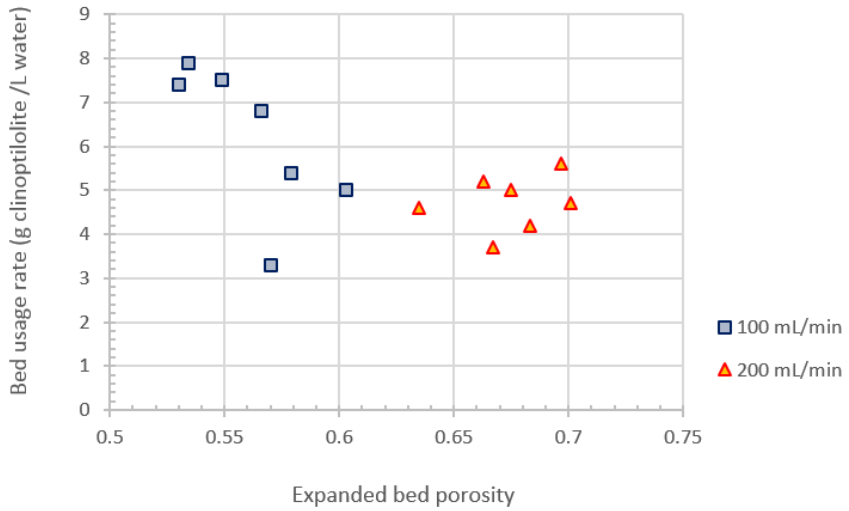

Figure 3. 26. Variation in bed usage rate with expanded bed porosity in polydisperse beds.

The graph in Figure 3.27 finally displays the two performance indicators used for the

evaluation and comparison of mixed size polydisperse beds operated in this study. As observed from the figure, only some of the particle compositions operated at 100 mL/min performed well similar to the performances obtained at 200 mL/min. On the other hand, ammonium exchange in polydisperse beds operated at a flow rate of 200 mL/min, resulted in lowered bed usage rates and higher breakthrough/total capacity ratios.

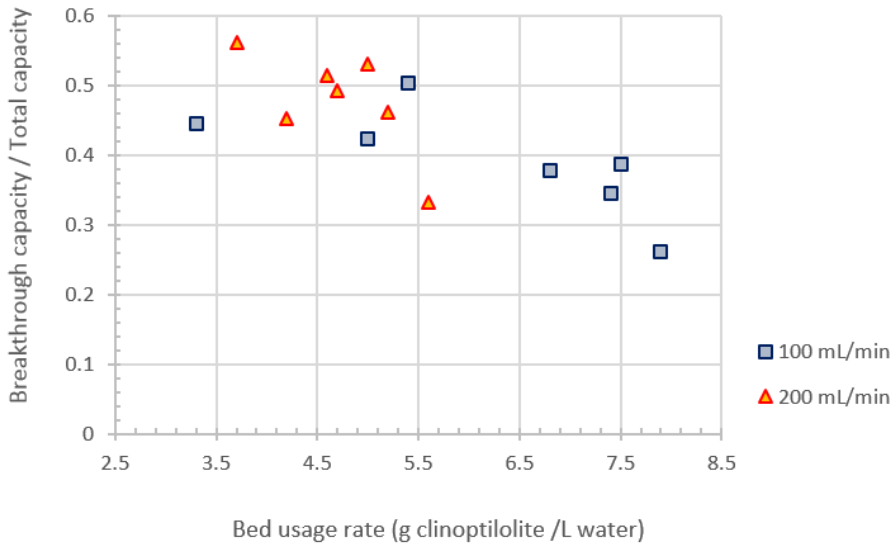

Figure 3. 27. Bed usage rate versus the ratio of breakthrough capacity to total capacity in polydisperse fluidized beds.

4. CONCLUSIONS

In this study, removal of ammonium ion from water in fluidized bed ion exchange columns of clinoptilolite was investigated experimentally. Four different fractions of clinoptilolite were prepared by sieving and by conditioning the surface of particles using sodium chloride. Four different monodispersed fluidized beds were operated at several different flow rates to investigate the effects of particle size and fluidization rate on ammonium exchange performance. 7 different compositions of polydisperse fluidized beds (four different compositions of binary beds, two different ternary beds and a bed containing all particle sizes together) were operated at two different flow rates to determine the effects of average particle size and mixing behaviors on ammonium exchange capacity. Same set of experiments were conducted at the same operating conditions to find the values of overall

mass transfer coefficients. All results of the experiments performed were evaluated using parameters: (i) ratio of breakthrough capacity to total (or exhaustion capacity), (ii) bed usage rate, and (iii) fractional capacity.

Main conclusions are summarized below:

- The ratio of breakthrough capacity to total capacity is increases when the column is efficiently. On the other hand, an improved performance is represented with a decreased value of bed usage rate.
- Increase in fluidization rate and employing particle mixtures of different sizes in the ion exchange bed were found to improve separation efficiencies of ammonium ion in clinoptilolite beds.
- Experiments with the fine sized particles in monodispersed beds, except the experiments performed at very high fluidization rate, resulted in low bed usage rates and a corresponding high breakthrough to total capacity ratios.
- For coarser particles, especially with at very fluidization rates, breakthrough capacity / total capacity ratios were very low with corresponding high bed usage rates, indicating the immediate leakage of NH_4^+ from the column effluent.
- Another set of experiments were conducted at the same operating conditions for determination of mass transfer coefficients. Binary and ternary beds had similar mass transfer coefficients which is also consistent with their ammonium exchange performance expressed as the ratio of breakthrough capacity to total capacity.
- Combinations of particle sizes with a high mass transfer coefficient, produced high breakthrough capacity to total capacities. Higher values of overall mass transfer coefficient was also observed for ion exchange experiments conducted at a high flow rate.
- Fractional capacity is the ratio of NH_4^+ exchange capacity of the bed remaining after breakthrough to NH_4^+ ion loading between time breakthrough and exhaustion time. A breakthrough curve with a lower value of F represents the better performance of that particle mixture than the others with higher F values. F values decreased in fluidized beds operated at higher flow rates.

Bed usage rate (with a unit of mass of clinoptilolite per liter of water) expresses how quickly the bed expends the available exchange sites during breakthrough. Increase in flow rate, with fluidization, resulted in a decrease in bed usage rates, which is an indicator of a better performance

REFERENCES

Alshameri, A., Yan, C., Al-Ani, Y., Dawood, S.A., Ibrahim, A., Zhou, C., Wang, H. (2014) An investigation into the adsorption removal of ammonium by salt activated Chinese (Hulaodu) natural zeolite: Kinetics, isotherms,and thermodynamics, Journal of the Taiwan Institute of Chemical Engineering, 45, 554-564.

Arslan, A., Veli, S. (2012) Zeolite 13X for adsorption of ammonium ions from aqueous solutions and hen slaughterhouse wastewaters, Journal of the Taiwan Institute of Chemical Engineering, 43, 393-398.

Chaudhari, S. V., Deshmukh, G. K. (2015) Fluidization Effect on Removal and Recovery of Palladium (II) From Wastewater by Chelated Ion Exchange Resin, Chemical Engineering Communications.

Demir, A., Günay, A. and Debik, E. (2002) Ammonium removal from aqueous solution by

ion-exchange using packed bed natural zeolite, African Journal Online, Vol28, No3.

Erbil, A., Soyer, E., Beler Baykal, B. (2011) Ammonium Ion Removal with a Natural Zeolite in Monodispersed and Segregated Fluidized Beds. Industrial and Engineering Chemistry Research, 50, 6391-6403.

Guo, J. (2015) Adsorption characteristics and mechanisms ofhigh-levels of ammonium from swine wastewater using natural and MgO modified zeolite, Desalination and Water Treatment, 1944-3986.

Haji, S., Al-Buqaishi, A. B., Bucheeri, A. A., Bu-Ali, Q., Al-Aseeri, M., Ahmed, S. (2015) The dynamics and equilibrium of ammoniumremoval from aqueous solution by Na-Y zeolite, Desalination and Water Treatment, 1944-3986..

Huang, H., Yang, L., Xue, Q., Liu, J., Hou, L., Ding, L. (2015) Removal of ammonium from swine wastewater by zeolite combined with chlorination for regeneration, Journal of Environmental Managment, 160, 333-341.

Huo, H., Lin, H., Dong, Y., Cheng, H., Wang, H., Cao, L. (2012) Ammonia-nitrogen and phosphates sorption from simulated reclaimed waters by modified clinoptilolite, Journal of Hazardous Material, 229-230, 292-297.

Kalaruban, M., Loganathan, P., Shim, W. G., Kandasamy, J., Naidu, G., Nguyen, V. T., Vigneswaran, S. (2016) Removing nitrate from water using iron-modified Dowex 21K XLT ionexchange resin: Batch and fluidised-bed adsorption studies, Seperation and Purification Technology, 158, 62-70.

Karadag, D., Koç, Y., Turan, M., Armagan, B. (2006) Removal of ammonium ion from aqueous solution usingnatural Turkish clinoptilolite, Journal of Hazardous Material, 136, 604-609.

Millar, J. G., Winnett, A., Thampson, T., Coupertwaite, J S. (2016) Equilibrium studies of ammonium exchange with Australian natural zeolites, Journal of Water Process Engineering, 9, 47-57.

Liao, L. Z., Chen, H., Zhu, B., Li, H. (2015) Combination of powdered activated carbon and powdered zeolite forenhancing ammonium removal in micro-polluted raw water, Chemosphere, 134, 127-132.

Lin, D-Q., Shi, W., Tong, H-F., J. A. X van de Sandt, E., den Boer, P., Ferreria. N. M. G., Yao, S-J. (2015) Evaluation and characterization of axial distribution in expanded bed: II.

Liquid mixing and local effective axial dispersion, Journal of Chromotography A, 1393, 65-72.

Lin, L., Lei, Z., Wang, L., Liu, X., Zhang, Y., Wan, C., Lee D. J., Tay, H. J. (2013) Adsorption mechanisms of high-levels of ammonium onto natural and NaCl- modified zeolites, Seperation and Purification technology, 103, 15-20.

Moltalvo, S., Guerrero, L., Borja, R., Sanchez, E., Milan, Z., Cortes, I., Angeles de la la Rubia, M. (2012) Application of natural zeolites in anaerobic digestion processes: A review, Applied Clay Science, 58, 125-133.

Saltalı, K., Sarı, A., Aydın, M. (2007) Removal of ammonium ion from aqueous solution by natural Turkish(Yıldızeli) zeolite for environmental quality, Journal of Hazardous Material, 141, 258-263.

Stylianou, M. A., Inglezakis, V. J., Loizidou, M. (2015) Comparison of Mn, Zn, and Cr removal in fluidized-and fixed-bed reactors by using clinoptilolite, Desalination and Water Treatment, 53:12, 3355-3362.

Zhou, L., Boyd E.C. (2014) Journal of the Taiwan Institute of Chemical Engineering, Aquaculture, 432, 252-257.

Wang, Y. F., Lin, F., Pang, Q. W. (2006) Ammonium exchange in aqueous solution using Chinesenatural clinoptilolite and modified zeolite, 142,160-164.

APPENDIX 3.2:

Table 1: Effluent concentration (mg/l), t/t_f ratio, C/C_0 and Bed Volumes related to Experiment1. 250-355 4.55 L / hour

BVs	t (min)	t/tf	C mg/L	C/Co
0.0	0	0.000	0	0.000
10.4	5	0.009	0.2795	0.011
31.2	15	0.026	0.2975	0.012
31.2	15	0.026	0.3005	0.012
41.6	20	0.034	0.3025	0.012
62.4	30	0.052	0.3045	0.012
72.8	35	0.060	0.3105	0.013
83.2	40	0.069	0.3145	0.013
93.5	45	0.078	0.316	0.013

103.9	50	0.086	0.322	0.013
124.7	60	0.103	0.3265	0.013
145.5	70	0.121	0.3305	0.013
166.3	80	0.138	0.365	0.015
187.1	90	0.155	0.4235	0.017
207.9	100	0.172	0.4275	0.017
228.7	110	0.190	0.4315	0.018
259.9	125	0.216	0.5445	0.022
291.0	140	0.241	0.625	0.025
311.8	150	0.259	0.6805	0.028
332.6	160	0.276	0.8945	0.036
353.4	170	0.293	1.245	0.051
374.2	180	0.310	1.435	0.058
395.0	190	0.328	1.635	0.066
415.8	200	0.345	1.785	0.073
436.6	210	0.362	2.185	0.089
457.3	220	0.379	2.775	0.113
467.7	225	0.388	3.255	0.132
498.9	240	0.414	4.715	0.192
540.5	260	0.448	5.795	0.236
582.1	280	0.483	6.49	0.264
602.9	290	0.500	8.535	0.347
623.6	300	0.517	8.99	0.365
665.2	320	0.552	10.9	0.443
686.0	330	0.569	11.65	0.474
706.8	340	0.586	12.45	0.506
727.6	350	0.603	13.15	0.535
738.0	355	0.612	13.9	0.565
758.8	365	0.629	14.95	0.608
779.6	375	0.647	15.9	0.646
790.0	380	0.655	16.8	0.683
821.1	395	0.681	17.65	0.717
841.9	405	0.698	18.45	0.750
862.7	415	0.716	19.1	0.776
873.1	420	0.724	19.75	0.803
893.9	430	0.741	20.15	0.819
925.1	445	0.767	20.65	0.839
945.9	455	0.784	20.75	0.843
966.7	465	0.802	21.1	0.858
997.8	480	0.828	21.6	0.878
1018.6	490	0.845	21.85	0.888
1039.4	500	0.862	22.25	0.904

1060.2	510	0.879	22.6	0.919
1081.0	520	0.897	23	0.935
1101.8	530	0.914	23.5	0.955
1122.6	540	0.931	23.9	0.972
1143.4	550	0.948	24	0.976
1164.1	560	0.966	24.25	0.986
1184.9	570	0.983	24.35	0.990
1205.7	580	1.000	24.6	1.000

Table 2: Effluent concentration (mg/l), t/t_f ratio, C/C_0 and Bed Volumes related to Experiment2. (250- 355 5.83 L/hour)

BVs	t (min)	t/tf	C mg/L	C/Co
0.0	0	0.000	0	0.000
10.4	5	0.009	0.2795	0.011
31.2	15	0.026	0.2975	0.012
31.2	15	0.026	0.3005	0.012
41.6	20	0.034	0.3025	0.012
62.4	30	0.052	0.3045	0.012
72.8	35	0.060	0.3105	0.013
83.2	40	0.069	0.3145	0.013
93.5	45	0.078	0.316	0.013
103.9	50	0.086	0.322	0.013
124.7	60	0.103	0.3265	0.013
145.5	70	0.121	0.3305	0.013

166.3	80	0.138	0.365	0.015
187.1	90	0.155	0.4235	0.017
207.9	100	0.172	0.4275	0.017
228.7	110	0.190	0.4315	0.018
259.9	125	0.216	0.5445	0.022
291.0	140	0.241	0.625	0.025
311.8	150	0.259	0.6805	0.028
332.6	160	0.276	0.8945	0.036
353.4	170	0.293	1.245	0.051
374.2	180	0.310	1.435	0.058
395.0	190	0.328	1.635	0.066
415.8	200	0.345	1.785	0.073
436.6	210	0.362	2.185	0.089
457.3	220	0.379	2.775	0.113
467.7	225	0.388	3.255	0.132
498.9	240	0.414	4.715	0.192
540.5	260	0.448	5.795	0.236
582.1	280	0.483	6.49	0.264
602.9	290	0.500	8.535	0.347
623.6	300	0.517	8.99	0.365
665.2	320	0.552	10.9	0.443
686.0	330	0.569	11.65	0.474
706.8	340	0.586	12.45	0.506
727.6	350	0.603	13.15	0.535
738.0	355	0.612	13.9	0.565
758.8	365	0.629	14.95	0.608
779.6	375	0.647	15.9	0.646
790.0	380	0.655	16.8	0.683
821.1	395	0.681	17.65	0.717
841.9	405	0.698	18.45	0.750
862.7	415	0.716	19.1	0.776
873.1	420	0.724	19.75	0.803
893.9	430	0.741	20.15	0.819
925.1	445	0.767	20.65	0.839
945.9	455	0.784	20.75	0.843
966.7	465	0.802	21.1	0.858
997.8	480	0.828	21.6	0.878
1018.6	490	0.845	21.85	0.888
1039.4	500	0.862	22.25	0.904
1060.2	510	0.879	22.6	0.919
1081.0	520	0.897	23	0.935
1101.8	530	0.914	23.5	0.955
1122.6	540	0.931	23.9	0.972
1143.4	550	0.948	24	0.976
1164.1	560	0.966	24.25	0.986

1184.9	570	0.983	24.35	0.990
1205.7	580	1.000	24.6	1.000

Table 3: Effluent concentration (mg/l), t/t_f ratio, C/C_0 and Bed Volumes related to Experiment3. (250- 355 7.138 L/hour).

BVs	t (min)	t/tf	C mg/L	C/Co
0.0	0	0.000	0	0.000
51.0	20	0.044	0.315	0.013
114.6	45	0.100	0.42	0.017
152.9	60	0.133	0.505	0.021
178.3	70	0.156	0.625	0.026
203.8	80	0.178	0.745	0.031
242.0	95	0.211	0.805	0.033
280.2	110	0.244	0.945	0.039
318.5	125	0.278	1.12	0.046
343.9	135	0.300	1.87	0.078
369.4	145	0.322	2.49	0.103
394.9	155	0.344	3.715	0.154
420.4	165	0.367	4.55	0.189
445.8	175	0.389	5.2	0.216
458.6	180	0.400	5.77	0.239
496.8	195	0.433	7.35	0.305
560.5	220	0.489	8.8	0.365
649.7	255	0.567	10.7	0.444
675.1	265	0.589	12.25	0.508
687.9	270	0.600	13.55	0.562
700.6	275	0.611	14.75	0.612
764.3	300	0.667	16.25	0.674
789.8	310	0.689	18.25	0.757
828.0	325	0.722	20.15	0.836
904.4	355	0.789	22.25	0.923
993.6	390	0.867	23.85	0.990
1146.5	450	1.000	24.1	1.000

Table 4: Effluent concentration (mg/l), t/tf ratio, C/C0 and Bed Volumes related to Experiment4. (250- 355 14.577 L/hour)

BVs	t (min)	t/tf	C mg/L	C/Co
0.0	0	0.000	0	0.000
78.0	15	0.050	0.415	0.017
156.0	30	0.100	0.55	0.022
234.0	45	0.150	0.81	0.032
312.0	60	0.200	1.21	0.048
390.0	75	0.250	2.51	0.100
468.0	90	0.300	4.1	0.163
546.0	105	0.350	4.76	0.189
624.0	120	0.400	5.45	0.217
676.0	130	0.433	6.46	0.257
754.0	145	0.483	8.88	0.353
832.0	160	0.533	11.3	0.449
910.1	175	0.583	14.45	0.575
988.1	190	0.633	16.3	0.648
1066.1	205	0.683	18.3	0.728
1144.1	220	0.733	19.5	0.775
1222.1	235	0.783	21.3	0.847
1274.1	245	0.817	23.55	0.936
1326.1	255	0.850	24.75	0.984
1378.1	265	0.883	25	0.994
1430.1	275	0.917	25.15	1.000
1560.1	300	1.000	25.15	1.000

Table 5: Effluent concentration (mg/l), t/tf ratio, C/C0 and Bed Volumes related to Experiment5. (250- 355 14.577 L/hour)

BVs	t (min)	t/tf	C mg/L	C/Co
0.0	0	0.000	0	0.000
78.6	15	0.052	0.581	0.018
131.0	25	0.086	0.6685	0.021
235.7	45	0.155	0.9655	0.030
314.3	60	0.207	1.505	0.047
419.1	80	0.276	3.215	0.100
523.9	100	0.345	5.025	0.156
602.5	115	0.397	8.01	0.248
654.9	125	0.431	12.2	0.378
733.4	140	0.483	14.95	0.464
812.0	155	0.534	19.1	0.592
890.6	170	0.586	23.1	0.716

995.4	190	0.655	24.95	0.774
1100.2	210	0.724	26.65	0.826
1152.5	220	0.759	28.15	0.873
1257.3	240	0.828	29.55	0.916
1309.7	250	0.862	30.15	0.935
1414.5	270	0.931	31.65	0.981
1466.9	280	0.966	31.95	0.991
1519.3	290	1.000	32.25	1.000

Table 6: Effluent concentration (mg/l), t/t_f ratio, C/C_0 and Bed Volumes related to Experiment6. (250- 355 17.4 L/hour)

BVs	t (min)	t/tf	C mg/L	C/Co
0.0	0	0.000	0	0.000
26.6	5	0.017	0.585	0.023
79.9	15	0.051	0.6365	0.025
106.5	20	0.068	0.6975	0.028
133.1	25	0.085	0.745	0.030
159.7	30	0.102	0.8315	0.033
213.0	40	0.136	0.908	0.036
239.6	45	0.153	1.125	0.045
292.8	55	0.186	1.885	0.075
372.7	70	0.237	1.99	0.079
399.3	75	0.254	3.53	0.141
452.6	85	0.288	5.855	0.234
505.8	95	0.322	7.515	0.300
532.4	100	0.339	8.75	0.349
585.7	110	0.373	10.55	0.421
638.9	120	0.407	13.35	0.533
692.2	130	0.441	15.35	0.613
718.8	135	0.458	16.55	0.661
798.7	150	0.508	17.85	0.713
878.5	165	0.559	18.05	0.721
931.8	175	0.593	19.25	0.768
1064.9	200	0.678	20.65	0.824
1118.1	210	0.712	21.4	0.854
1144.8	215	0.729	22.25	0.888
1437.6	270	0.915	23.95	0.956
1570.7	295	1.000	25.05	1.000

Table 7: Effluent concentration (mg/l), t/t_f ratio, C/C_0 and Bed Volumes related to Experiment7. (250- 355 19.2 L/hour)

BVs	t (min)	t/tf	C mg/L	C/Co
0.0	0	0.000	0	0.000
31.0	5	0.016	0.715	0.028
93.1	15	0.048	0.825	0.033
124.2	20	0.065	0.985	0.039
155.2	25	0.081	1.325	0.052
186.3	30	0.097	1.845	0.073
248.3	40	0.129	1.995	0.079
279.4	45	0.145	2.13	0.084
341.5	55	0.177	2.465	0.097
434.6	70	0.226	4.12	0.163
465.6	75	0.242	6.405	0.253
527.7	85	0.274	8.795	0.348
589.8	95	0.306	9.35	0.370
620.9	100	0.323	10.255	0.405
683.0	110	0.355	12.88	0.509
745.0	120	0.387	14.695	0.581
807.1	130	0.419	15.965	0.631
838.2	135	0.435	16.555	0.654
931.3	150	0.484	18.25	0.721
1024.4	165	0.532	20.045	0.792
1086.5	175	0.565	20.99	0.830
1148.6	185	0.597	21.55	0.852
1241.7	200	0.645	22.35	0.883
1303.8	210	0.677	22.85	0.903
1334.9	215	0.694	23.35	0.923
1490.1	240	0.774	24.05	0.951
1676.3	270	0.871	24.65	0.974
1831.6	295	0.952	24.9	0.984
1862.6	300	0.968	25.15	0.994
1893.6	305	0.984	25.25	0.998
1924.7	310	1.000	25.3	1.000

Table 8: Effluent concentration (mg/l), t/tf ratio, C/C0 and Bed Volumes related to Experiment8. (250-355 17.42 L/hour)

BVs	t (min)	t/tf	C mg/L	C/Co
0.0	0	0.000	0	0.000
102.8	15	0.067	1.65	0.068
205.5	30	0.133	3.43	0.141
308.3	45	0.200	6.86	0.281
376.8	55	0.244	8.83	0.362
445.3	65	0.289	10.4	0.426
513.8	75	0.333	12.5	0.512
616.6	90	0.400	14.3	0.586
753.6	110	0.489	16.75	0.686
822.1	120	0.533	17.9	0.734
890.6	130	0.578	19.15	0.785
1061.9	155	0.689	20.75	0.850
1096.2	160	0.711	22.1	0.906
1233.2	180	0.800	23.5	0.963
1335.9	195	0.867	24.25	0.994
1438.7	210	0.933	24.4	1.000
1541.5	225	1.000	24.4	1.000

Table 9: Effluent concentration (mg/l), t/tf ratio, C/C0 and Bed Volumes related to Experiment9. (425-500 23.04 L/hour)

BVs	t (min)	t/tf	C mg/L	C/Co
0.0	0	0.000	0	0.000
42.1	5	0.016	2.22	0.088
84.2	10	0.031	2.41	0.096
126.4	15	0.047	2.71	0.108
168.5	20	0.063	2.915	0.116
252.7	30	0.094	3.22	0.128
337.0	40	0.125	3.42	0.136
421.2	50	0.156	3.61	0.144
505.5	60	0.188	3.86	0.153
631.9	75	0.234	4.25	0.169
758.2	90	0.281	6.29	0.250
884.6	105	0.328	7.09	0.282
1011.0	120	0.375	9.81	0.390
1095.2	130	0.406	10.485	0.417
1179.5	140	0.438	11.2	0.445

1263.7	150	0.469	13.3	0.529
1390.1	165	0.516	16.12	0.641
1474.4	175	0.547	18.05	0.718
1685.0	200	0.625	20.71	0.823
1895.6	225	0.703	21.45	0.853
2064.1	245	0.766	22.6	0.899
2316.9	275	0.859	24.15	0.960
2359.0	280	0.875	24.45	0.972
2527.5	300	0.938	24.625	0.979
2611.7	310	0.969	25.025	0.995
2696.0	320	1.000	25.15	1.000

Table 10: Effluent concentration (mg/l), t/tf ratio, C/C_0 and Bed Volumes related to Experiment10. (500-600 4.548 L/hour)

BVs	t (min)	t/tf	C mg/L	C/Co
0.0	0	0.000	0	0.000
8.6	5	0.009	0.137	0.005
17.2	10	0.017	0.233	0.009
43.1	25	0.043	0.432	0.017
51.7	30	0.051	0.681	0.026
68.9	40	0.068	1.52	0.058
86.2	50	0.085	1.62	0.062
94.8	55	0.094	1.69	0.065
112.0	65	0.111	1.82	0.070
120.7	70	0.120	1.93	0.074
129.3	75	0.128	2.01	0.077
137.9	80	0.137	2.37	0.091
155.1	90	0.154	2.42	0.093
215.5	125	0.214	3.2	0.123
249.9	145	0.248	4.66	0.179
267.2	155	0.265	4.89	0.188
301.6	175	0.299	6.13	0.236
318.9	185	0.316	6.4	0.246
336.1	195	0.333	7.21	0.277
353.4	205	0.350	8.35	0.321
379.2	220	0.376	9.82	0.378
387.8	225	0.385	10.6	0.408
405.1	235	0.402	11.8	0.454
413.7	240	0.410	12	0.462
439.5	255	0.436	12.5	0.481
456.8	265	0.453	12.8	0.492
525.7	305	0.521	14.1	0.542
560.2	325	0.556	16.5	0.635
594.7	345	0.590	17.9	0.688
611.9	355	0.607	18.4	0.708
620.5	360	0.615	18.7	0.719
637.8	370	0.632	19.1	0.735
655.0	380	0.650	19.3	0.742
672.2	390	0.667	19.5	0.750
715.3	415	0.709	20.1	0.773
732.6	425	0.726	20.7	0.796
749.8	435	0.744	21.3	0.819
767.0	445	0.761	21.7	0.835
836.0	485	0.829	22.7	0.873
844.6	490	0.838	23.1	0.888

870.5	505	0.863	23.8	0.915
896.3	520	0.889	24.1	0.927
930.8	540	0.923	25	0.962
948.0	550	0.940	25.4	0.977
965.3	560	0.957	25.6	0.985
982.5	570	0.974	25.7	0.988
1008.4	585	1.000	26	1.000

Table 11: Effluent concentration (mg/l), t/t_f ratio, C/C_0 and Bed Volumes related to Experiment11. (500-600 5.9 L/hour)

BVs	t (min)	t/tf	C mg/L	C/Co
0.0	0	0.000	0	0.000
11.1	5	0.010	0.6245	0.026
22.1	10	0.020	0.7135	0.029
33.2	15	0.030	0.7325	0.030
44.3	20	0.040	0.7325	0.030
55.4	25	0.051	0.8015	0.033
66.4	30	0.061	0.9335	0.038
99.7	45	0.091	1.315	0.054
110.7	50	0.101	1.575	0.065
121.8	55	0.111	1.955	0.080
143.9	65	0.131	3.255	0.133
166.1	75	0.152	3.345	0.137
188.2	85	0.172	5.175	0.212
221.5	100	0.202	5.245	0.215
243.6	110	0.222	6.125	0.251
265.7	120	0.242	6.395	0.262
287.9	130	0.263	6.585	0.270
310.0	140	0.283	7.375	0.302
321.1	145	0.293	7.715	0.316
343.3	155	0.313	9.895	0.406
365.4	165	0.333	10.305	0.422
398.6	180	0.364	11.45	0.469
420.8	190	0.384	13.3	0.545
442.9	200	0.404	14.695	0.602
465.1	210	0.424	15.205	0.623
509.3	230	0.465	16.305	0.668
531.5	240	0.485	17.005	0.697
564.7	255	0.515	17.395	0.713
586.9	265	0.535	18.05	0.740
609.0	275	0.556	18.3	0.750

631.1	285	0.576	18.85	0.773
686.5	310	0.626	19.2	0.787
719.7	325	0.657	19.8	0.811
730.8	330	0.667	20.05	0.822
764.0	345	0.697	20.55	0.842
797.2	360	0.727	20.75	0.850
819.4	370	0.747	21.2	0.869
852.6	385	0.778	21.55	0.883
874.7	395	0.798	22.05	0.904
885.8	400	0.808	22.45	0.920
941.2	425	0.859	22.8	0.934
985.5	445	0.899	23.05	0.945
1018.7	460	0.929	23.65	0.969
1096.2	495	1.000	24.4	1.000

Table 12: Effluent concentration (mg/l), t/tf ratio, C/C0 and Bed Volumes related to Experiment12. (500-600 6.9 L/h)

BVs	t (min)	t/tf	C mg/L	C/Co
0.0	0	0.000	0	0.000
98.7	15	0.036	3.285	0.128
197.4	30	0.072	6.98	0.272
296.1	45	0.108	8.93	0.348
394.8	60	0.145	12.8	0.499
493.5	75	0.181	15.65	0.610
592.2	90	0.217	16.15	0.630
690.9	105	0.253	18.85	0.735
855.4	130	0.313	21.05	0.821
954.1	145	0.349	22.25	0.867
1052.8	160	0.386	23.05	0.899
1151.5	175	0.422	23.35	0.910
1250.2	190	0.458	23.65	0.922
1381.8	210	0.506	23.75	0.926
1480.5	225	0.542	24.35	0.949
1579.2	240	0.578	24.6	0.959
1710.8	260	0.627	24.65	0.961
1809.5	275	0.663	25.15	0.981
1908.2	290	0.699	25.25	0.984
2006.9	305	0.735	25.35	0.988
2039.8	310	0.747	25.4	0.990
2138.5	325	0.783	25.4	0.990
2171.4	330	0.795	25.45	0.992
2270.1	345	0.831	25.5	0.994
2368.8	360	0.867	25.55	0.996

2467.5	375	0.904	25.6	0.998
2730.8	415	1.000	25.65	1.000

Table 13: Effluent concentration (mg/l), t/t_f ratio, C/C_0 and Bed Volumes related to Experiment12. 500-600 7.138 L / hour

BVs	t (min)	t/tf	C mg/L	C/Co
0.0	0	0.000	0	0.000
13.5	5	0.014	0.855	0.034
27.0	10	0.029	1.3	0.052
54.0	20	0.057	1.985	0.079
81.0	30	0.086	1.985	0.079
108.0	40	0.114	3.3	0.131
135.0	50	0.143	4.62	0.183
148.5	55	0.157	5.36	0.213
162.0	60	0.171	6.05	0.240
189.0	70	0.200	6.53	0.259
202.5	75	0.214	7.11	0.282
216.0	80	0.229	8.31	0.330
243.0	90	0.257	9.055	0.359
270.0	100	0.286	11.31	0.449
297.0	110	0.314	12.5	0.496
324.0	120	0.343	13.555	0.538
351.0	130	0.371	14.68	0.583
378.0	140	0.400	16.55	0.657
391.5	145	0.414	17.205	0.683
405.0	150	0.429	19.5	0.774
459.0	170	0.486	20.05	0.796
526.5	195	0.557	21.1	0.837
567.0	210	0.600	21.85	0.867
607.5	225	0.643	22.4	0.889
648.0	240	0.686	23.45	0.931
688.5	255	0.729	23.75	0.942
729.0	270	0.771	24.05	0.954
783.0	290	0.829	24.65	0.978
823.5	305	0.871	24.9	0.988
864.0	320	0.914	25.05	0.994
904.5	335	0.957	25.15	0.998
945.0	350	1.000	25.2	1.000

Table 14: Effluent concentration (mg/l), t/t_f ratio, C/C_0 and Bed Volumes related to Experiment13. 500-600 17.4L / hour

BVs	t (min)	t/tf	C mg/L	C/Co
0.0	0	0.000	0	0.000
98.7	15	0.036	3.285	0.128
197.4	30	0.072	6.98	0.272
296.1	45	0.108	8.93	0.348
394.8	60	0.145	12.8	0.499
493.5	75	0.181	15.65	0.610
592.2	90	0.217	16.15	0.630
690.9	105	0.253	18.85	0.735
855.4	130	0.313	21.05	0.821
954.1	145	0.349	22.25	0.867
1052.8	160	0.386	23.05	0.899
1151.5	175	0.422	23.35	0.910
1250.2	190	0.458	23.65	0.922
1381.8	210	0.506	23.75	0.926
1480.5	225	0.542	24.35	0.949
1579.2	240	0.578	24.6	0.959
1710.8	260	0.627	24.65	0.961
1809.5	275	0.663	25.15	0.981
1908.2	290	0.699	25.25	0.984
2006.9	305	0.735	25.35	0.988
2039.8	310	0.747	25.4	0.990
2138.5	325	0.783	25.4	0.990
2171.4	330	0.795	25.45	0.992
2270.1	345	0.831	25.5	0.994
2368.8	360	0.867	25.55	0.996
2467.5	375	0.904	25.6	0.998
2730.8	415	1.000	25.65	1.000

APPENDIX 3.3:

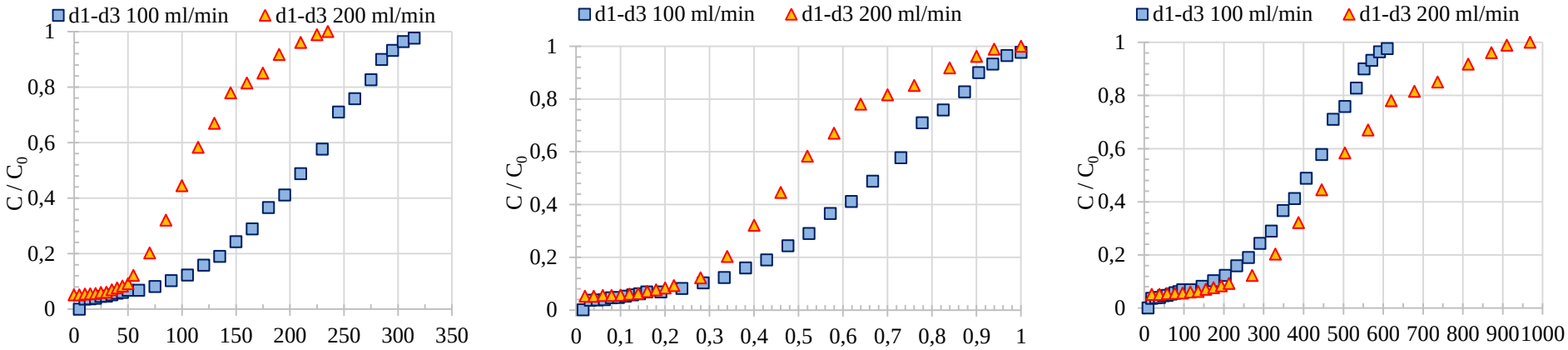

Material: 250-355 & 425-500 um mixture. Breakthrough curves with respect to time, t/tf, and BV for 100 and 200 mL/min.

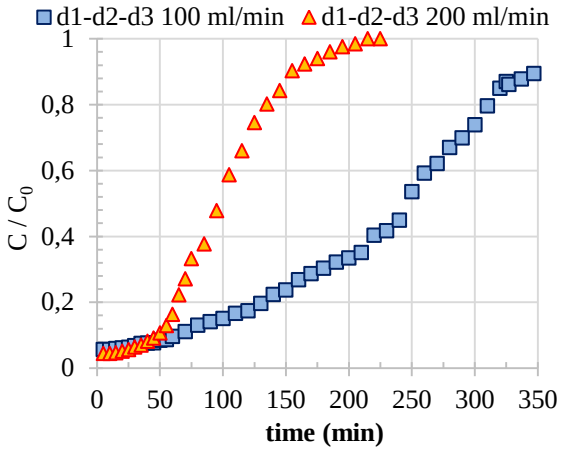

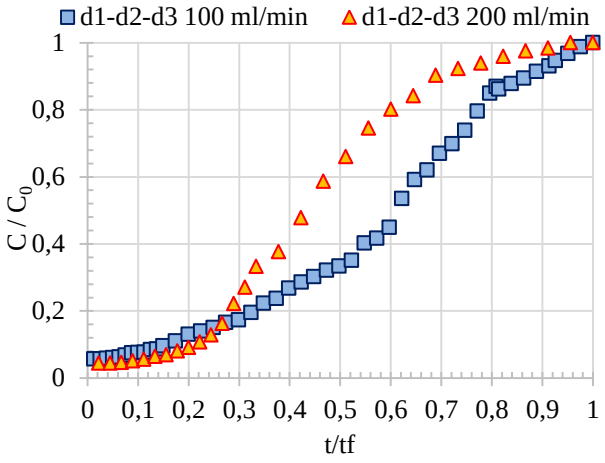

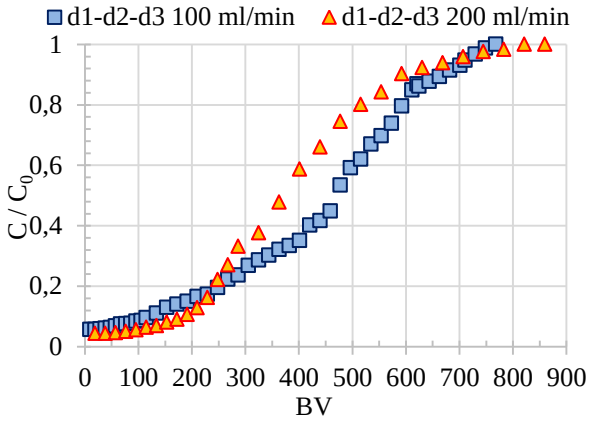

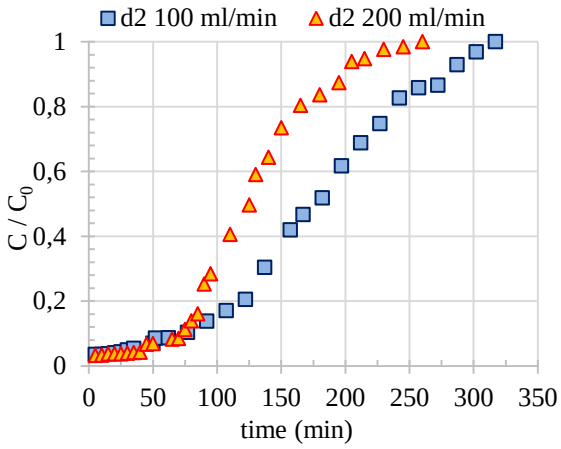

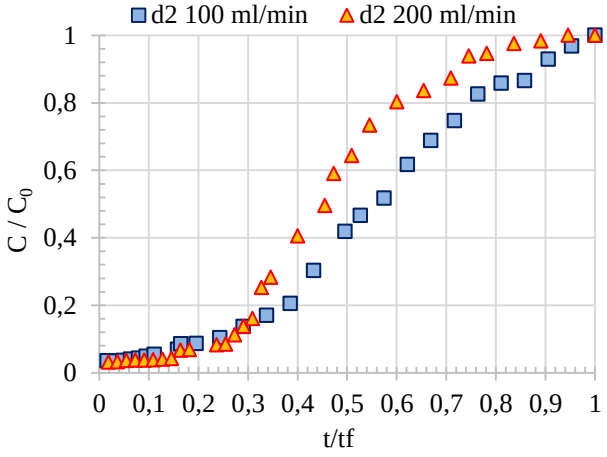

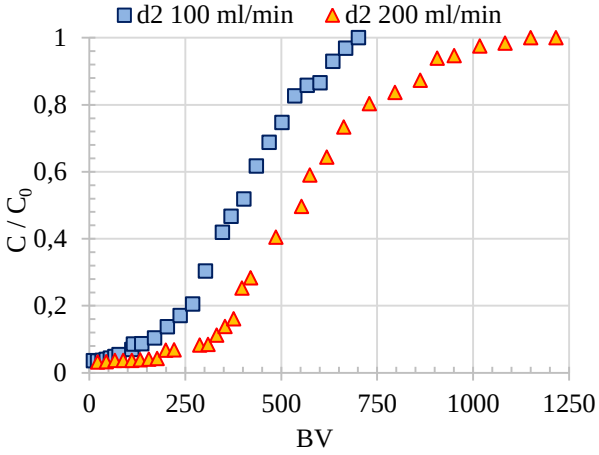

Material: 355-425 um mixture. Breakthrough curves with respect to time, t/tf, V for 100 and 200 mL/min.

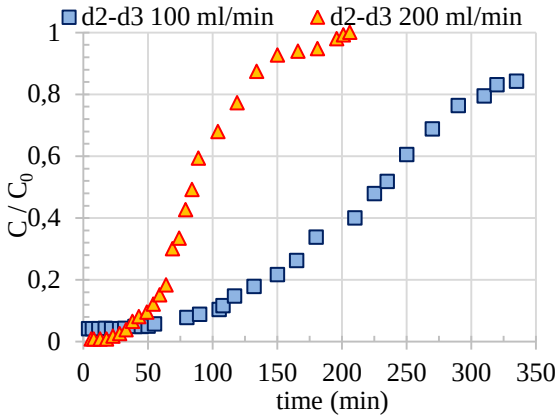

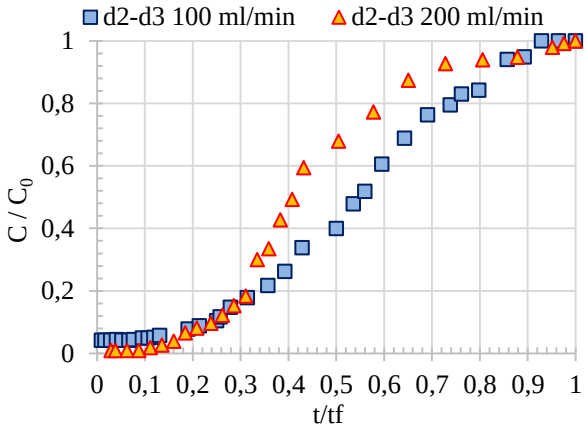

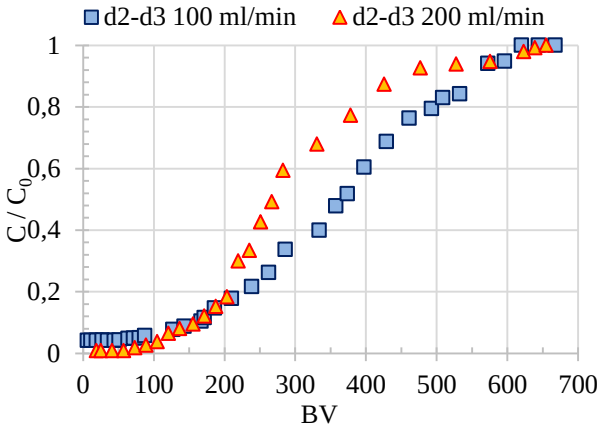

Material: 355-425 & 425-500 um mixture. Breakthrough curves with respect to time, t/tf, and BV for 100 and 200 mL/min.

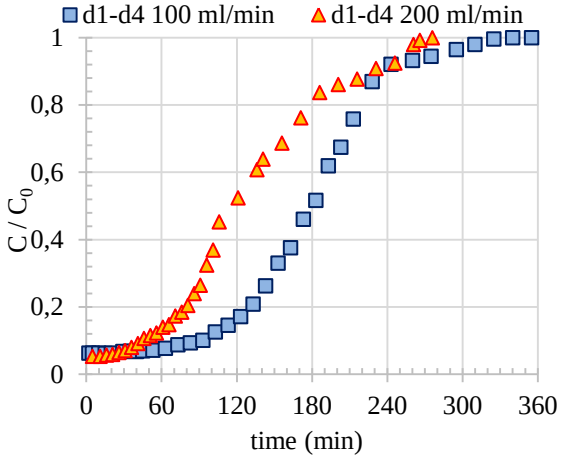

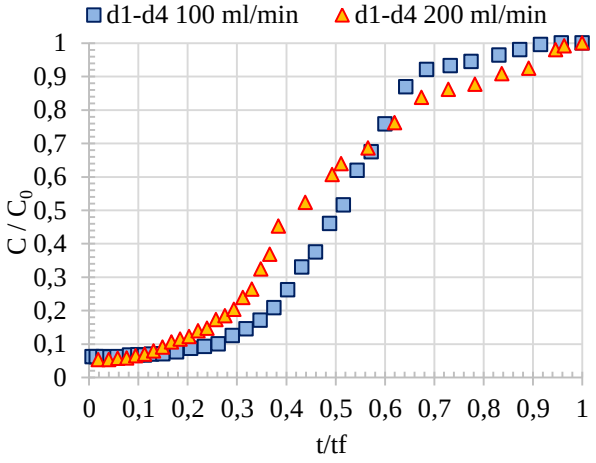

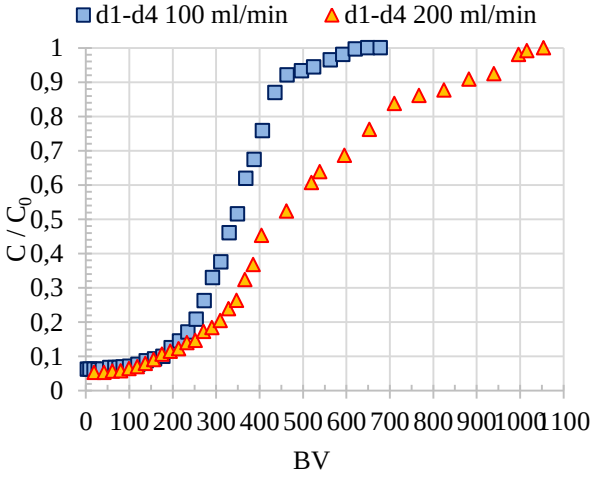

Material: 250-355 & 355-425um mixture. Breakthrough curves with respect to time, t/tf, and BV for 100 and 200 mL/min.

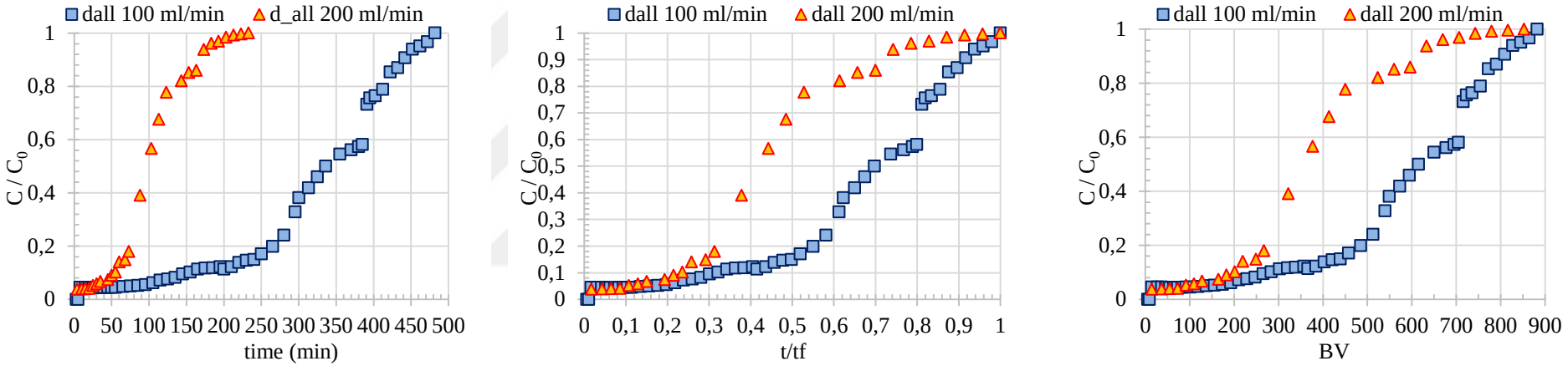

Material: 250-355 & 355-425 & 425-500 & 500-600 um mixture. Breakthr. curves with respect to time, t/tf, and BV for 100 and 200 mL/min.

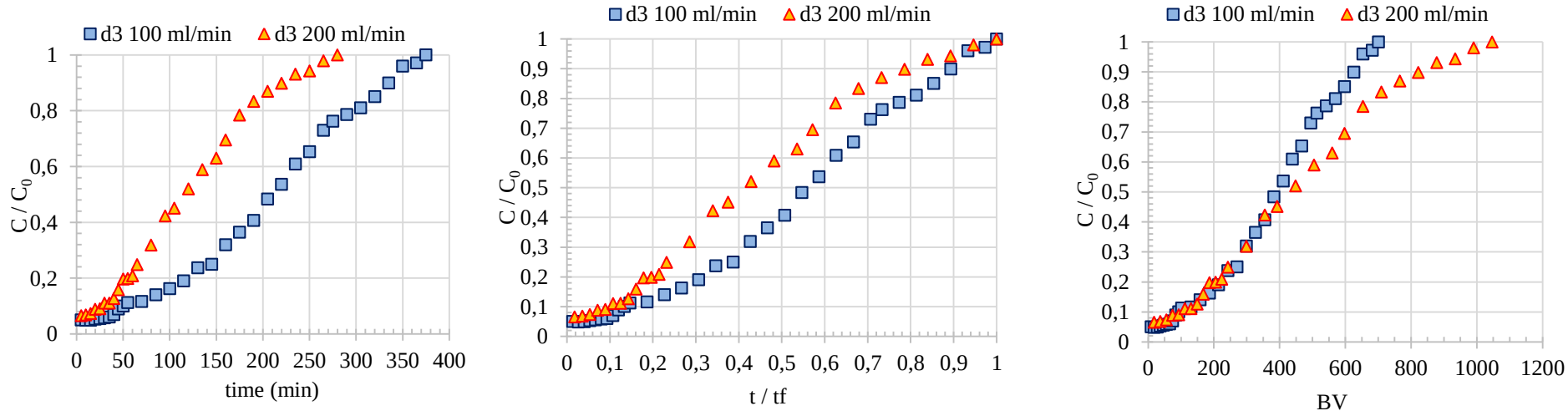

Material: 425-500 um mixture. Breakthrough curves with respect to time, t/tf, and BV for 100 and 200 mL/min.

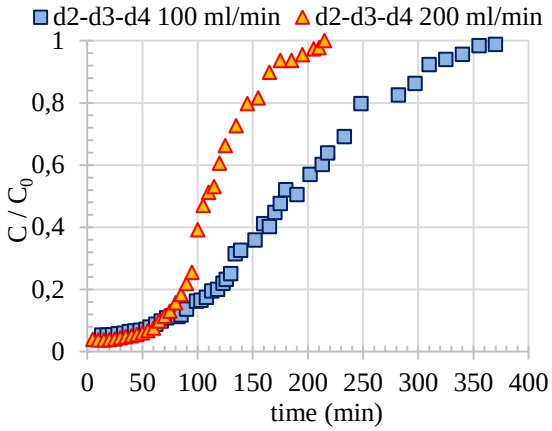

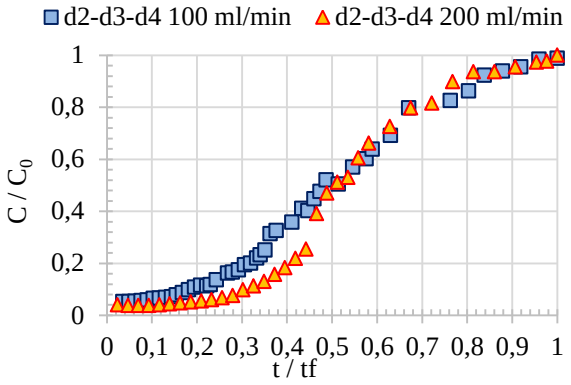

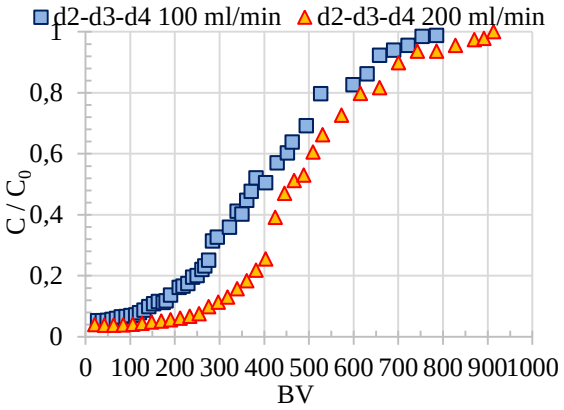

Material: 355-425 & 425-500 & 500-600 um mixture. Breakthrough curves with respect to time, t/tf, and BV for 100 and 200 mL/min.

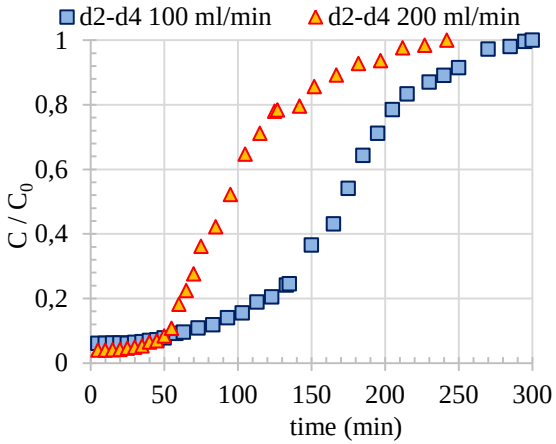

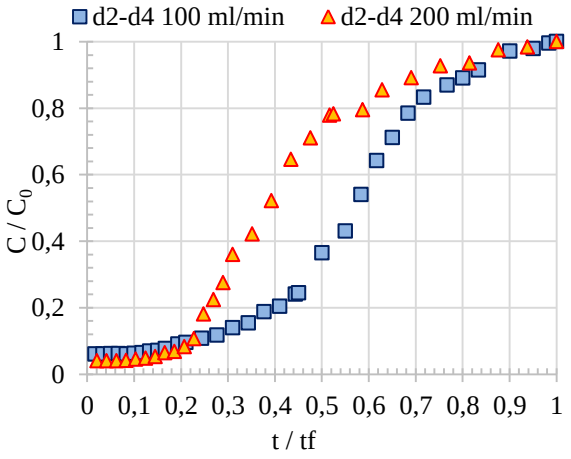

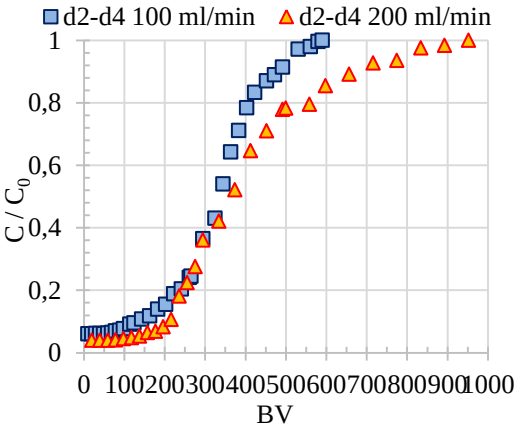

CURRICULUM VITAE

Name Surname : Gülay ARSLAN

Birth Location and Date : Gaziosmanpaşa / ISTANBUL, 15.01.1990

E-mail : gulay.arslan@marmara.edu.tr

Education

Degree	Department / Program	University / High School	Graduation Year
High School	Applied science and technology	Gaziosmanpaşa Anatolian High School	2008
University	Environmental Engineering	Istanbul University	2012

Work Experience

Year	Firm / Foundation	Duty / Responsibility
2012	Marmara University	Research Assistant

Conference Proceeding

Arslan G. , Soyer E. , "Ion Exchange Assisted Membrane Filtration Using Clinoptilolite Powders", International Porous and Powder Materials Symposium and Exhibition, PPM 2015, İZMİR, TÜRKIYE, 15-18 Eylül 2015, pp 299-302.